nectin is involved in neurite growth during development (Matthiessen et al., 1989) and plays an important role in the spinal cord development in humans (Krolo et al., 1998). The expression of fibronectin is regionally and developmentally regulated in the brain, and its presence is relatively minor in the normal CNS (Jones, 1996). However, once injuries occur, its expression is dramatically increased (Hoke and Silver, 1996; Pasinetti et al., 1993). Fibronectin also exists at high concentrations in the blood plasma, and a breakdown of the blood-brain barrier (BBB) should result in an increase in its local concentration in the CNS. Thus, it is highly plausible that the increased fibronectin may somehow upregulate $P2X_4$ receptors in microglia.

The signaling pathway(s) by which fibronectin promotes $P2X_4$ upregulation is currently under investigation. Microglia possess functional β1 integrin, which is one of the receptors for fibronectin, and they undergo firm adhesion, activation (Milner and Campbell, 2002, 2003), and proliferation (Nasu-Tada et al., 2005) through this molecule, presumably by regulating intracellular signaling cascades. Thus, fibronectin-to-integrin-mediated signals may be critical for the $P2X_4$ receptor upregulation. It is interesting that, among various P2 receptors expressed in microglia, i.e., $P2X_7$, $P2Y_2$, $P2Y_6$, and $P2Y_{12}$ receptors, only the $P2X_4$ receptor is upregulated by fibronectin (Fig. 1). This result suggests that the $P2X_4$ receptor gene may undergo unique transcriptional regulation by the linkage of fibronectin to integrin.

The Correlation Between Spinal Fibronectin and Mechanical Allodynia in Rats

We showed that spinal fibronectin was upregulated after the nerve injury. Several lines of evidence indicate that fibronectin is directly upregulated at the site of injuries in the PNS (Lefcort et al., 1992; Martini, 1994; Vogelezang et al., 1999) and CNS (Hoke and Silver, 1996; Pasinetti et al., 1993); but to our knowledge, there has been no report demonstrating that fibronectin is upregulated at a distal region, i.e., in the CNS, after peripheral nerve injury. The clinical signs of allodynia induced in rat in the Chung model become evident by 3-day post operation and the phenotype reached the maximum by 1-week post operation. The concomitant upregulation of the microglial $P2X_4$ receptors, which is observed only on the ipsilateral side of the spinal cord, follows the same time-course profile (Tsuda et al., 2003). In this study, the expression of the spinal fibronectin was strongly augmented, but again only on the ipsilateral side, during the course of mechanical allodynia, and the expression pattern was also similar to the time-course of the above. Therefore, our results strongly suggest that the upregulation of the ipsilateral fibronectin correlates both with the induction of allodynia and with the upregulation of the microglial $P2X_4$ receptor. Since it is usually observed that mechanical allodynia spans several weeks, it is still necessary for us to investigate the relationship between the upregulation of fibronectin and chronic allodynia. Our data so far postulate that fibronectin may be involved in the onset of the disease, most likely by initiating the upregulation of the microglial $P2X_4$ receptor.

Since fibronectin is known to be present at a high concentration in the blood plasma, it is plausible that the peripheral nerve injury caused a local breakdown of the central BBB, and that the breakdown resulted in a transfer of the blood plasma fibronectin into the corresponding part of the CNS. In a cortical cold-injury model, fibronectin was found to leak from blood vessels (Nag et al., 2001; Nourhaghighi et al., 2003); but in another report, such exudation was not seen after spinal cord injury (Farooque et al., 1992). Interestingly, the plasma fibronectin expression is known to be elevated after tissue injury (Thompson et al., 1992). Recently, plasma fibronectin was reported to support neuronal survival and reduce bran injury following transient focal cerebral ischemia, but it was not essential for skin-wound healing and hemostasis (Sakai et al., 2001). Alternatively, fibronectin may be synthesized by neuronal and glial cells in the CNS. Fibronectin is a vital molecule in neural development and regeneration (Venstrom and Reichardt, 1993), and astrocytes are known to synthesize and release fibronectin (Jiang et al., 1994; Matthiessen et al., 1989; Price and Hynes, 1985). A recent report by Tom et al. (2004) revealed that astroglial-associated fibronectin plays a key role in axonal regeneration in the white matter and, indeed, astrocytes produce and release fibronectin in response to ATP stimulation (unpublished observation). However, so far we have not identified the source of the upregulated fibronectin, and the mechanism by which fibronectin is upregulated after peripheral nerve injury remains to be clarified.

The effect of fibronectin was further highlighted by the experiment involving intrathecal transfer. In our previous study (Tsuda et al., 2003), microglia that were treated with 50 μM ATP could induce mechanical allodynia when they were intrathecally transferred into a normal rat. Microglia that were cultured on fibronectin and treated with 5 μM ATP were capable of inducing mechanical allodynia. In contrast, control microglia were not able to induce mechanical allodynia at that ATP concentration. The result suggests that fibronectin lowered the threshold of pain sensation. Fifty μM of ATP was adequate to cause mechanical allodynia by intrathecal transfer in both groups, suggesting that the effect of microglia in causing allodynia in response to ATP stimulation is saturated at an ATP concentration of 50 μM. Although microglia have other P2 receptors, i.e., $P2X_7$, $P2Y_2$, $P2Y_6$, and $P2Y_{12}$ receptors, only $P2X_4$ receptors are involved in the induction of mechanical allodynia (Tsuda et al., 2003). Interestingly, fibronectin upregulated only $P2X_4$ receptors but downregulated other P2 receptors on microglia at the mRNA level (Fig. 1). Thus, the involvement of other microglial P2 receptors in pain sensation, the threshold of which was lowered by fibronectin, would be negligible. Altogether, the results suggest that microglia with upregulated $P2X_4$ receptors by fibronectin treatment were able to transduce signals that lead to allodynia at a lower concentration of ATP.

In summary, we demonstrated that fibronectin induces the upregulation of $P2X_4$ receptors on microglia in vitro, and that fibronectin is increased in the spinal cord in vivo when mechanical allodynia is induced after peripheral nerve injury. When microglia are intrathecally administered into normal rats, they induce mechanical allodynia only if pre-stimulated with ATP (Tsuda et al., 2003). Our ex vivo experiments showed that fibronectin lowers the ATP concentration that is necessary for microglia to induce this pain behavior. Although both the signaling pathway by which fibronectin promotes $P2X_4$ upregulation and the source of increased fibronectin are currently under investigation, all these findings suggest that the upregulation of spinal fibronectin may be involved in the onset mechanism of mechanical allodynia after nerve injury.

ACKNOWLEDGMENTS

We thank Dr. Ohno for continuous encouragement. This study was partly supported by an MF-16 grant from The National Institute of Biomedical Innovation, a grant from Uehara Memorial Foundation, a grant-in-aid for Scientific Research (B), for Young Scientists (A) and on Priority Areas (A) from the Ministry of Education, Science, Sports and culture of Japan.

REFERENCES

Adams JC, Watt FM. 1993. Regulation of development and differentiation by the extracellular matrix. Development 117:1183–1198.

Cavaliere F, Florenzano F, Amadio S, Fusco FR, Viscomi MT, D'Ambrosi N, Vacca F, Sancesario G, Bernardi G, Molinari M, et al. 2003. Up-regulation of P2X2, P2X4 receptor and ischemic cell death: prevention by P2 antagonists. Neuroscience 120:85–98.

Farooque M, Zhang Y, Holtz A, Olsson Y. 1992. Exudation of fibronectin and albumin after spinal cord injury in rats. Acta Neuropathol (Berl) 84:613–620.

Hoke A, Silver J. 1996. Proteoglycans and other repulsive molecules in glial boundaries during development and regeneration of the nervous system. Prog Brain Res 108:149–163.

Hynes RO. 1992. Integrins: versatility, modulation, and signaling in cell adhesion. Cell 69:11–25.

Inoue K. 2002. Microglial activation by purines and pyrimidines. Glia 40:156–163.

Jiang B, Liou GI, Behzadian MA, Caldwell RB. 1994. Astrocytes modulate retinal vasculogenesis: effects on fibronectin expression. J Cell Sci 107:2499–2508.

Jones LS. 1996. Integrins: possible functions in the adult CNS. Trends Neurosci 19:68–72.

Krolo M, Vilovic K, Sapunar D, Vrdoljak E, Saraga-Babic M. 1998. Fibronectin expression in the developing human spinal cord, nerves, and ganglia. Croat Med J 39:386–391.

Le KT, Babinski K, Seguela P. 1998. Central P2X4 and P2X6 channel subunits coassemble into a novel heteromeric ATP receptor. J Neurosci 18:7152–7159.

Lefcort F, Venstrom K, McDonald JA, Reichardt LF. 1992. Regulation of expression of fibronectin and its receptor, alpha 5 beta 1, during development and regeneration of peripheral nerve. Development 116: 767–782.

Martini R. 1994. Expression and functional roles of neural cell surface molecules and extracellular matrix components during development and regeneration of peripheral nerves. J Neurocytol 23:1–28.

Matthiessen HP, Schmalenbach C, Muller HW. 1989. Astroglia-released neurite growth-inducing activity for embryonic hippocampal neurons is associated with laminin bound in a sulfated complex and free fibronectin. Glia 2:177–188.

Milner R, Campbell IL. 2002. Cytokines regulate microglial adhesion to laminin and astrocyte extracellular matrix via protein kinase C-dependent activation of the alpha6beta1 integrin. J Neurosci 22: 1562–1572.

Milner R, Campbell IL. 2003. The extracellular matrix and cytokines regulate microglial integrin expression and activation. J Immunol 170: 3850–3858.

Nag S, Picard P, Stewart DJ. 2001. Expression of nitric oxide synthases and nitrotyrosine during blood-brain barrier breakdown and repair after cold injury. Lab Invest 81:41–49.

Nakajima K, Shimojo M, Hamanoue M, Ishiura S, Sugita H, Kohsaka S. 1992. Identification of elastase as a secretory protease from cultured rat microglia. J Neurochem 58:1401–1408.

Nasu-Tada K, Koizumi S, Inoue K. 2005. Involvement of beta1 integrin in microglial chemotaxis and proliferation on fibronectin: different regulations by ADP through PKA. Glia 52:98–107.

Nourhaghighi N, Teichert-Kuliszewska K, Davis J, Stewart DJ, Nag S. 2003. Altered expression of angiopoietins during blood-brain barrier breakdown and angiogenesis. Lab Invest 83:1211–1222.

Pasinetti GM, Nichols NR, Tocco G, Morgan T, Laping N, Finch CE. 1993. Transforming growth factor beta 1 and fibronectin messenger RNA in rat brain: responses to injury and cell-type localization. Neuroscience 54:893–907.

Price J, Hynes RO. 1985. Astrocytes in culture synthesize and secrete a variant form of fibronectin. J Neurosci 5:2205–2211.

Raghow R. 1994. The role of extracellular matrix in postinflammatory wound healing and fibrosis. Faseb J 8:823–831.

Ralevic V, Burnstock G. 1998. Receptors for purines and pyrimidines. Pharmacol Rev 50:413–492.

Sakai T, Johnson KJ, Murozono M, Sakai K, Magnuson MA, Wieloch T, Cronberg T, Isshiki A, Erickson HP, Fassler R. 2001. Plasma fibronectin supports neuronal survival and reduces brain injury following transient focal cerebral ischemia but is not essential for skin-wound healing and hemostasis. Nat Med 7:324–330.

Sasaki Y, Hoshi M, Akazawa C, Nakamura Y, Tsuzuki H, Inoue K, Kohsaka S. 2003. Selective expression of Gi/o-coupled ATP receptor P2Y12 in microglia in rat brain. Glia 44:242–250.

Soto F, Garcia-Guzman M, Gomez-Hernandez JM, Hollmann M, Karschin C, Stuhmer W. 1996. P2X4: an ATP-activated ionotropic receptor cloned from rat brain. Proc Natl Acad Sci USA 93:3684–3688.

Thompson PN, Cho E, Blumenstock FA, Shah DM, Saba TM. 1992. Rebound elevation of fibronectin after tissue injury and ischemia: role of fibronectin synthesis. Am J Physiol 263:G437–G445.

Tom VJ, Doller CM, Malouf AT, Silver J. 2004. Astrocyte-associated fibronectin is critical for axonal regeneration in adult white matter. J Neurosci 24:9282–9290.

Tsuda M, Inoue K, Salter MW. 2005. Neuropathic pain and spinal microglia: a big problem from molecules in "small" glia. Trends Neurosci 28:101–107.

Tsuda M, Shigemoto-Mogami Y, Koizumi S, Mizokoshi A, Kohsaka S, Salter MW, Inoue K. 2003. P2X4 receptors induced in spinal microglia gate tactile allodynia after nerve injury. Nature 424:778–783.

Venstrom KA, Reichardt LF. 1993. Extracellular matrix. 2: Role of extracellular matrix molecules and their receptors in the nervous system. Faseb J 7:996–1003.

Vogelezang MG, Scherer SS, Fawcett JW, ffrench-Constant C. 1999. Regulation of fibronectin alternative splicing during peripheral nerve repair. J Neurosci Res 56:323–333.

Yeung D, Kharidia R, Brown SC, Gorecki DC. 2004. Enhanced expression of the P2X4 receptor in Duchenne muscular dystrophy correlates with macrophage invasion. Neurobiol Dis 15:212–220.

Zhang FL, Luo L, Gustafson E, Palmer K, Qiao X, Fan X, Yang S, Laz TM, Bayne M, Monsma F, Jr. 2002. P2Y(13): identification and characterization of a novel Galphai-coupled ADP receptor from human and mouse. J Pharmacol Exp Ther 301:705–713.

Direct excitation of deep dorsal horn neurones in the rat spinal cord by the activation of postsynaptic P2X receptors

Hiroaki Shiokawa[1], Terumasa Nakatsuka[1,2], Hidemasa Furue[1], Makoto Tsuda[3], Toshihiko Katafuchi[1], Kazuhide Inoue[3] and Megumu Yoshimura[1]

[1]*Department of Integrative Physiology, Graduate School of Medical Sciences, Kyushu University, Fukuoka 812-8582, Japan*
[2]*Department of Physiology, Faculty of Medicine, Saga University, Saga 849-8501, Japan*
[3]*Department of Molecular and System Pharmacology, Graduate School of Pharmaceutical Sciences, Kyushu University, Fukuoka 812-8582, Japan*

ATP mediates somatosensory transmission in the spinal cord through the activation of P2X receptors. Nonetheless, the functional significance of postsynaptic P2X receptors in spinal deep dorsal horn neurones is still not yet well understood. Using the whole-cell patch-clamp technique, we investigated whether the activation of postsynaptic P2X receptors can modulate the synaptic transmission in lamina V neurones of postnatal day (P) 9–12 spinal cord slices. At a holding potential of −70 mV, ATPγS (100 μM), a nonhydrolysable ATP analogue, generated an inward current, which was resistant to tetrodotoxin (1 μM) in 61% of the lamina V neurones. The ATPγS-induced inward current was accompanied by a significant increase in the frequency of glutamatergic miniature excitatory postsynaptic currents (mEPSCs) in the majority of lamina V neurones. The ATPγS-induced inward current was not reproduced by P2Y receptor agonists, UTP (100 μM), UDP (100 μM), and 2-methylthio ADP (100 μM), and it was also not affected by the addition of guanosine-5′-*O*-(2-thiodiphosphate) (GDPβS) into the pipette solution, thus suggesting that ionotropic P2X receptors were activated by ATPγS instead of metabotropic P2Y receptors. On the other hand, α,β-methylene ATP (100 μM) did not change any membrane current, but instead increased the mEPSC frequency in the majority of lamina V neurones. The ATPγS-induced inward current was suppressed by pyridoxalphosphate-6-azophenyl-2′,4′-disulphonic acid (PPADS) (10 μM), but not by trinitrophenyl-ATP (TNP-ATP) (1 μM). Furthermore, we found that ATPγS (100 μM) produced a clear inward current which was observed in all lamina V neurones over P16 spinal cord slices, in contrast to P9–12. These results indicate that distinct subtypes of P2X receptors were functionally expressed at the post- and presynaptic sites in lamina V neurones, both of which may contribute to the hyperexcitability of lamina V in a different manner. In addition, the data relating to the developmental increase in the functional P2X receptors suggest that purinergic signalling may thus be more common in somatosensory transmission with maturation.

(Received 1 March 2006; accepted after revision 12 April 2006; first published online 13 April 2006)
Corresponding author T. Nakatsuka: Department of Physiology, Faculty of Medicine, Saga University, Saga 849-8501, Japan. Email: nakatsuk@cc.saga-u.ac.jp

Extracellular ATP plays a crucial role in nociceptive transmission in the central and peripheral nervous systems (Burnstock & Wood, 1996; Hamilton & McMahon, 2000; Chizh & Illes, 2001; Kennedy *et al.* 2003; Liu & Salter, 2005). ATP receptors are divided into two classes, ionotropic P2X receptors (Khakh, 2001; North, 2002) and G-protein-coupled metabotropic P2Y receptors (von Kügelgen & Wetter, 2000). To date, seven P2X receptor subunits ($P2X_1$ to $P2X_7$) have been cloned (North & Surprenant, 2000). Each P2X subunit has two transmembrane domains with a cysteine-rich extracellular loop, which contains an ATP-binding site. A functional P2X receptor is composed of three or more P2X subunits, forming a pore structure that is permeable to cations including Ca^{2+}. Assembled from seven P2X subunits, at least 11 subtypes of functional P2X receptors can thus be formed in heterologous expression systems. These 11 P2X receptors are homomeric $P2X_1$ to $P2X_7$ receptors, heteromeric $P2X_{1/5}$, $P2X_{2/3}$, $P2X_{2/6}$ and $P2X_{4/6}$ (Khakh *et al.* 2001; North, 2002).

The spinal dorsal horn (DH) is the first site in the central nervous system where somatosensory information is

H. Shiokawa and T. Nakatsuka contributed equally to this work.

DOI: 10.1113/jphysiol.2006.108613

processed. Deep DH (DDH) neurones transmit a variety of sensory inputs, including nociceptive and non-nociceptive inputs, while superficial DH (SDH) neurones receive nociceptive specific sensory inputs (Willis & Coggeshall, 1991). Six of seven P2X receptor subunits ($P2X_1$ to $P2X_6$) are expressed in the DH (Collo *et al.* 1996; Vulchanova *et al.* 1997; Guo *et al.* 1999). Multiple subtypes of P2X receptors were located at the central terminals of primary afferents that innervate onto DH neurones (Vulchanova *et al.* 1997; Guo *et al.* 1999). The activation of these distinct P2X receptors enhances glutamate release in different manners (Nakatsuka & Gu, 2001; Nakatsuka *et al.* 2003; Chen & Gu, 2005). The modulation of glutamate release by presynaptic P2X receptors is mainly transient in lamina II neurones (Nakatsuka *et al.* 2003). In contrast, P2X receptor-mediated modulation of glutamate release is long-lasting in lamina I and lamina V neurones (Nakatsuka & Gu, 2001; Nakatsuka *et al.* 2003; Chen & Gu, 2005). Moreover, the activation of presynaptic P2X receptors modulates not only excitatory, but also the inhibitory synaptic transmission in SDH neurones (Li & Perl, 1995; Li *et al.* 1998; Hugel & Schlichter, 2000; Rhee *et al.* 2000). The activation of certain types of presynaptic P2X receptors also increases the GABA and glycine release onto SDH neurones (Hugel & Schlichter, 2000; Rhee *et al.* 2000).

Although these functional roles of presynaptic P2X receptors have been well established, little is known about the postsynaptic P2X receptors in the DH. Jahr & Jessell (1983) first reported the action of ATP on cultured DH neurones. In spinal cord slice preparations, the bath application of ATP also induces inward currents in lamina II neurones of spinal cord slices (Li & Perl, 1995). However, it is not clear whether the ATP-evoked depolarization or inward current in these studies are mediated by postsynaptic P2X receptors in DH neurones or secondary responses. In acutely dissociated neurones from the SDH, ATP induces inward currents (Bardoni *et al.* 1997; Rhee *et al.* 2000) and evokes Ca^{2+} transients (Bardoni *et al.* 1997). In addition, excitatory postsynaptic currents (EPSCs) cannot be completely blocked by glutamate receptor antagonists, but they can be blocked by the addition of P2X receptor antagonists in a small population of lamina II neurones (Bardoni *et al.* 1997). These results suggest that postsynaptic P2X receptors in a sub-population of SDH neurones can mediate somatosensory transmission in the spinal cord. However, the possible roles of postsynaptic P2X receptors in DDH neurones have never been documented up to now. DDH neurones, especially lamina V neurones, generate long-lasting afterdischarges in response to nociceptive inputs (Woolf & King, 1987). As a result, the development of hyperactivity in DDH neurones is involved in a variety of pathological pain sensations (Willis & Coggeshall, 1991; Mao *et al.* 1992). Therefore, the aim of this study was to evaluate the effects of postsynaptic P2X receptors on synaptic transmission in DDH neurones of spinal cord slices.

Methods

All the experimental procedures involving the use of animals were approved of by the Ethics Committee on Animal Experiments, Kyushu University, and were in accordance with the UK Animals (Scientific Procedures) Act 1986 and associated guidelines.

Spinal cord slice preparation

The methods used to obtain rat spinal cord slice preparations have been previously described (Nakatsuka *et al.* 1999). In brief, Sprague-Dawley rats at a postnatal age 9–19 days were deeply anaesthetized with urethane ($1.2\,g\,kg^{-1}$, intraperitoneal), and then a lumbosacral laminectomy was performed. The lumbosacral spinal cord (L1–S3) was removed and placed in preoxygenated Krebs solution at 1–3°C. Immediately after the removal of the spinal cord, the rats were given an overdose of urethane and then were killed by exsanguination. The pia-arachnoid membrane was removed after cutting all the ventral and dorsal roots near the root entry zone. The spinal cord was mounted on a vibratome and then a 500-μm-thick transverse slice was cut. The slice was placed in the recording chamber, which had a volume of 0.5 ml, and placed on the stage of an upright IR-DIC microscope (Axio Skop 2, Carl Zeiss). Next, the slice was superfused at a rate of $5\,ml\,min^{-1}$ with Krebs solution saturated with 95% O_2 and 5% CO_2 at room temperature. The Krebs solution contained (mM) 117 NaCl, 3.6 KCl, 2.5 $CaCl_2$, 1.2 $MgCl_2$, 1.2 NaH_2PO_4, 25 $NaHCO_3$ and 11 glucose.

Patch-clamp recordings from DDH neurones

The lamina regions were identified with a 5× objective lens, and individual neurones were identified with a 40× objective lens under IR-DIC microscope. The microscope was coupled with a CCD camera (XC-EI30, SONY) and a video monitor screen. Whole-cell patch-clamp recordings were made from lamina V neurones with patch-pipette electrodes having a resistance of 4–8 MΩ (Nakatsuka & Gu, 2001). The composition of the patch-pipette solution was as follows (mM): 135 potassium gluconate, 5 KCl, 0.5 $CaCl_2$, 2 $MgCl_2$, 5 EGTA, 5 Hepes, 5 ATP-Mg, pH 7.2. Guanosine-5′-*O*-(2-thiodiphosphate) (GDPβS) was added at a concentration of 2 mM to the patch-pipette solution when necessary. The signals were acquired with an amplifier (EPC-9, HEKA). The data were digitized with an A/D converter (MacLab, ADInstruments), stored on a personal computer using a data acquisition program (Chart 3.6.9, ADInstruments),

and then were analysed using a software program (AxoGraph 4.6, Axon Instruments). The lamina V neurones were viable for up to 12 h in slices perfused with pre-oxygenated Krebs solution. However, all the recordings described here were obtained within 8 h. The firing patterns of the lamina V neurones were determined in current clamp by passing 1 s long depolarizing pulses through the recording electrode from a holding potential of −60 mV. Whole-cell patch-clamp recordings were stable for up to 3 h. A holding membrane potential of −70 mV was used unless otherwise mentioned.

Cell identification

The location and morphological features of the recorded cells were further confirmed in some instances by an intrasomatic injection of neurobiotin (0.2% in recording electrode solution). After terminating the electrophysiological recordings, the slices were fixed overnight with 4% paraformaldehyde in 0.1 M phosphate buffer (PB, pH 7.4) at 4°C and rinsed in 0.1 M PB. Visualization of neurobiotin-labelled cells was performed by diaminobenzidine (DAB)-based histochemistry. Free-floating sections were incubated in Vectastain (Elite kit; Vector Laboratories) according to the manufacturer's protocol. The peroxidase activity was revealed with DAB in the presence of hydrogen peroxide, and sections were mounted on gelatinized slides. The sections were viewed and photographed with a microscope (Eclipse E600, Nikon).

Application of drugs

Drugs were dissolved in Krebs solution and applied by perfusion via a three-way stopcock without any change in the perfusion rate. The time necessary for the solution to flow from the stopcock to the surface of the spinal cord slice was approximately 20 s. The drugs used in this study were adenosine 5′-*O*-(3-thiotriphosphate) (ATPγS), α,β-methylene ATP (αβmeATP), uridine 5′-triphosphate (UTP), uridine 5′-diphosphate (UDP), 2 methyltio ADP (2meSADP), pyridoxalphosphate-6-azophenyl-2′,4′-disulphonic acid (PPADS), trinitrophenyl-ATP (TNP-ATP), GDPβS, and baclofen from Sigma (St Louis, MO, USA); tetrodotoxin (TTX) from Wako (Osaka, Japan); 6-cyano-7-nitroquinoxaline-2,3-dion (CNQX) and D(−)-2-amino-5-phosphonovaleric acid (APV) were purchased from Tocris Cookson (Bristol, UK).

Statistical analysis

All numerical data were expressed as the mean ± standard error (S.E.M.). Statistical significance was determined as $P < 0.05$ using Student's paired t test to compare the amplitude of the inward currents and as $P < 0.05$ using non-parametric Kolomogorov–Smirnov's test to compare the frequency of the miniature excitatory postsynaptic currents (mEPSCs). In the electrophysiological data, n refers to the number of neurones studied.

Results

Dual effect of ATPγS on synaptic transmission in DDH neurones

Whole-cell patch-clamp recordings were performed from lamina V neurones of P9–12 spinal cord slices. Stable recording was obtained from a single lamina V neurone for up to 4 h. In the current-clamp mode, all neurones were classified into tonic firing, showing regular firing throughout the current pulse (Fig. 1*B*). The majority of lamina V neurones possessed the morphological features of a rounded soma with dendrites branching off dorsally and ventrally (Fig. 1*A*). In the voltage-clamp mode, perfusion with ATPγS (100 μM) for 1 min induced an inward current in 67 out of 109 lamina V neurones at a holding potential of −70 mV (Fig. 1*C*). The average amplitude of the peak currents induced by ATPγS (100 μM) was 11.0 ± 0.8 pA ($n = 67$). In the presence of CNQX (20 μM) and APV (50 μM), ATPγS (100 μM) also produced an inward current (Fig. 1*C*). In the same lamina V neurones examined, the average amplitude of the peak currents induced by ATPγS in the presence of CNQX and APV was 14.4 ± 8.3 pA, and was not significantly different from that in the absence of CNQX and APV (15.6 ± 9.3 pA, $n = 4$). In 55 out of 67 neurones, the ATPγS-induced inward current was accompanied by a significant increase in the frequency of glutamatergic sEPSCs (Fig. 2*A*). The average increase in the sEPSC frequency was 200 ± 14% of control ($n = 55$, Fig. 2*B*). The bath application of ATPγS (100 μM) did not change any membrane current in the remaining 42 neurones tested, but significantly increased the frequency of glutamatergic sEPSCs in 29 neurones (Fig. 2*C*). The average increase in the sEPSC frequency was 184 ± 11% of control ($n = 29$, Fig. 2*D*). When ATPγS (100 μM) was applied repeatedly at 10 min intervals, it produced similar inward currents with almost the same amplitude ($n = 4$, Fig. 3*A*). Moreover, these ATPγS-induced currents were resistant to TTX (1 μM, Fig. 3*B*). In the same lamina V neurones, the average amplitude of the ATPγS-induced currents in the presence of TTX was 104 ± 4% of that in the absence of TTX ($n = 5$). When examined in the concentration range of 10–300 μM, the ATPγS-induced inward currents were enhanced in amplitude with increasing concentrations (Fig. 4*A* and *B*). We further examined the changes in the membrane conductance of the ATPγS-induced currents in the presence of TTX (1 μM) (Fig. 4*C*). Voltage steps

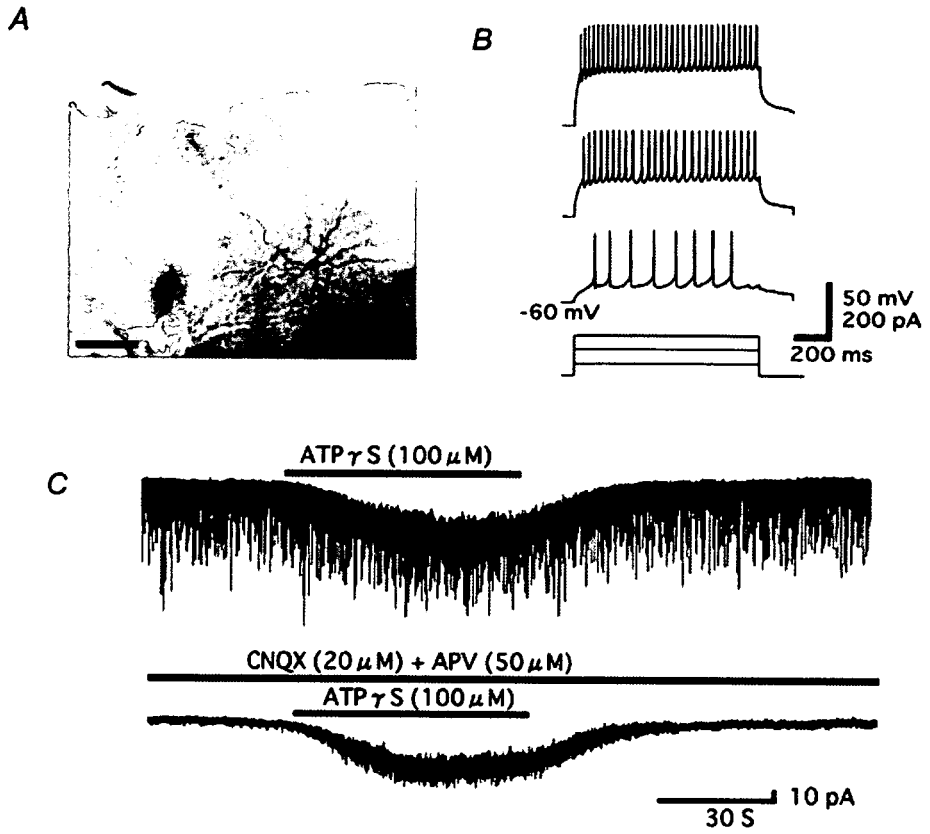

Figure 1. ATPγS excites lamina V neurones in spinal cord slices
A, a recorded lamina V neurone identified with an intracellular injection with neurobiotin. Scale bar is 100 μm. *B*, all lamina V neurones examined displayed tonic firing in response to depolarizing current injection of 143.6 pA (upper trace), 93.6 pA (middle trace), or 43.6 pA (lower trace) in current-clamp mode. *C*, in voltage-clamp mode, ATPγS (100 μM) produced a clear inward current at a holding potential of −70 mV (upper trace). In the presence of CNQX (20 μM) and APV (50 μM), ATPγS (100 μM) still induced an inward current without a significant decrease in amplitude in the same lamina V neurone (lower trace).

(duration: >50 ms) from a holding potential of −70 mV to voltages ranging from −40–40 mV in steps of 10 mV were given to lamina V neurones in the absence or presence of ATPγS. Figure 4*D* demonstrates the relationships between the step voltage and the steady current at the end of its pulse in the absence (s) and presence (●) of ATPγS (100 μM). The net ATPγS-induced current (○) estimated from a difference between the two

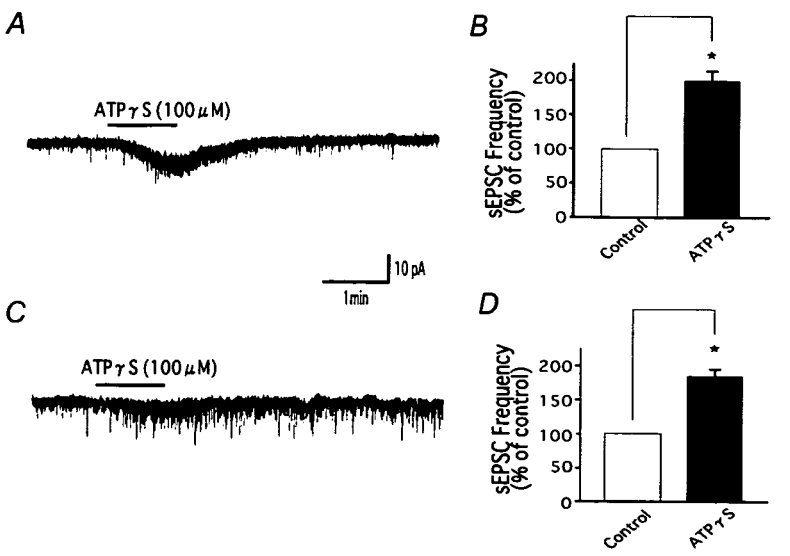

Figure 2. Post- or presynaptic effect of ATPγS in lamina V neurones
A, bath application of ATPγS (100 μM) for 1 min induced a clear inward current associated with a marked increase in the sEPSC frequency in a P9–12 lamina V neurone. The ATPγS-induced inward current was observed in approximately 60% of lamina V neurones examined. *B*, a summary of relative sEPSC frequency before (control) and during application of ATPγS in lamina V neurones which exhibited the ATPγS-induced inward current (*$P < 0.05$). *C*, ATPγS (100 μM) did not change any membrane current, but largely increased the sEPSC frequency in a P9–P12 lamina V neurone. *D*, a summary of the relative sEPSC frequency before (control) and during the application of ATPγS in lamina V neurones which did not exhibit any ATPγS-induced inward current (*$P < 0.05$). Error bars S.E.M.

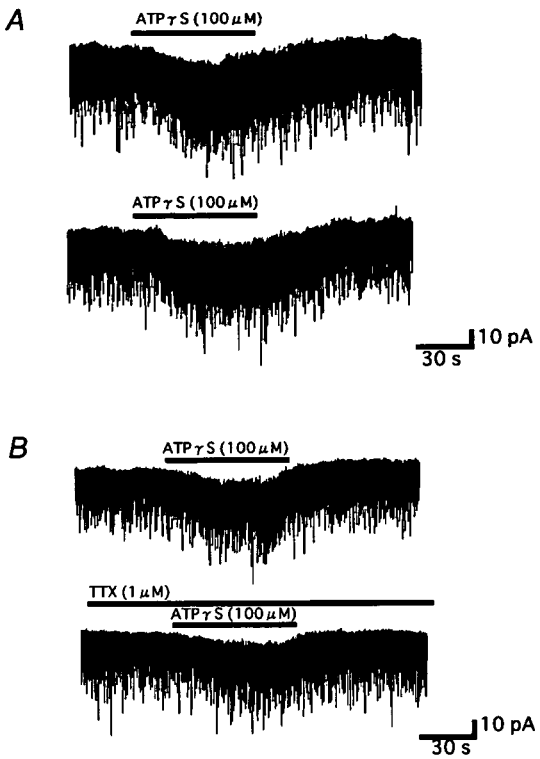

Figure 3. ATPγS repeatedly induces an inward current in lamina V neurones
A, when ATPγS was repeatedly applied at 10 min intervals, it produced a similar inward current (upper trace, the first application of ATPγS; lower trace, the second application of ATPγS). *B*, in the presence of TTX (1 μM), ATPγS induced an inward current without any decrease in the amplitude (upper trace, in the absence of TTX; lower trace, in the presence of TTX).

currents exhibited a reversal potential of -1.3 ± 4.7 mV ($n = 4$), which was compatible with the activation of a non-selective cation conductance.

Effects of P2Y receptor agonists

To determine whether the ATPγS-induced inward current is mediated by metabotropic P2Y receptors, the effect of P2Y receptor agonists on membrane currents was observed in the lamina V neurones. The bath application of UTP (100 μM), an agonist for $P2Y_2$ and $P2Y_4$ receptors, for 1 min affected neither the membrane currents nor the glutamatergic excitatory synaptic transmission in lamina V neurones where ATPγS induced an inward currents ($n = 4$, Fig. 5*A*). UDP (100 μM), an agonist for $P2Y_6$ receptors, and 2meSADP (100 μM), an agonist for $P2Y_1$, $P2Y_{12}$ and $P2Y_{13}$, also changed neither membrane currents nor glutamatergic excitatory synaptic transmission in lamina V neurones ($n = 4$, Fig. 5*A*).

To examine the involvement of intracellular G-proteins in the ATPγS-induced inward current, GDPβS (2 mM), a nonhydrolysable analogue of GDP that competitively inhibits G-proteins, was added to the pipette solution. When ATPγS (100 μM) was applied just after establishing the whole-cell configuration with pipettes containing potassium gluconate and GDPβS, an inward current was observed ($n = 4$). When ATPγS was again applied 1 h later, it produced similar inward currents with almost the same amplitude (96.5 ± 13.8% of the control, $P > 0.05$, Fig. 5*B* and *C*). Under the same conditions, the baclofen-induced

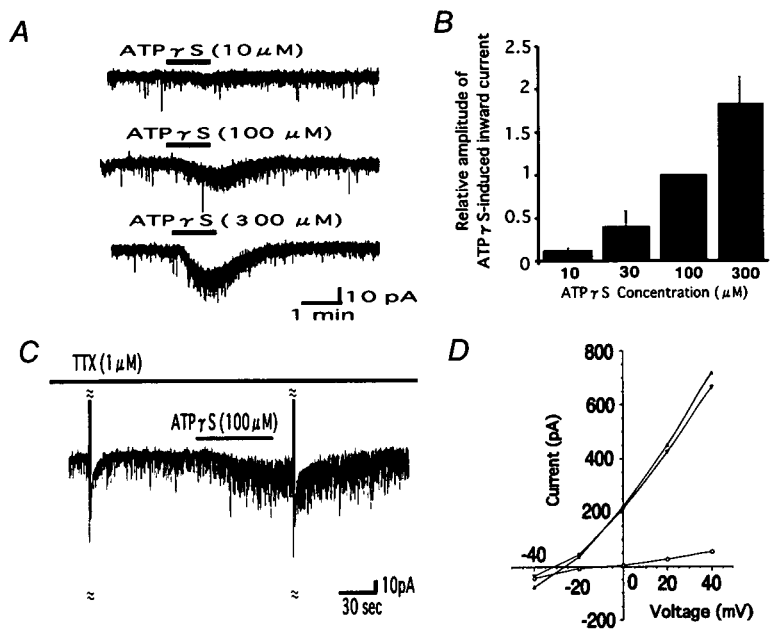

Figure 4. Dose and voltage dependency of the ATPγS-induced inward current
A, the ATPγS-induced inward currents showed an enhanced amplitude with increasing concentrations. *B*, normalized amplitude of the ATPγS-induced inward currents was plotted against the ATPγS concentration. The vertical bar indicates S.E.M. ($n = 3$–6). *C*, to examine a change in membrane conductance of the ATPγS-induced currents, a voltage step (duration, >50 ms) from −60 mV to + 40 mV in steps of 10 mV was given to lamina V neurones before and during application of ATPγS (100 μM) in the presence of TTX (1 μM). *D*, the amplitude of membrane currents in response to voltage pulses from −60 mV to +40 mV was plotted against voltages in the absence (▲) and presence (●) of ATPγS (100 μM). The current–voltage relationship for net ATPγS current was estimated based on the difference between the current responses in the absence and presence of ATPγS (○).

outward currents were significantly suppressed by the addition of GDPβS into the pipette solution in four lamina V neurones examined (29.4 ± 14.2% of the control, Fig. 5*C*). These results indicated the absence of a relationship with the activation of intracellular G-proteins. As a result, the ATPγS-induced inward current was mediated by ionotropic P2X receptors, rather than metabotropic P2Y receptors.

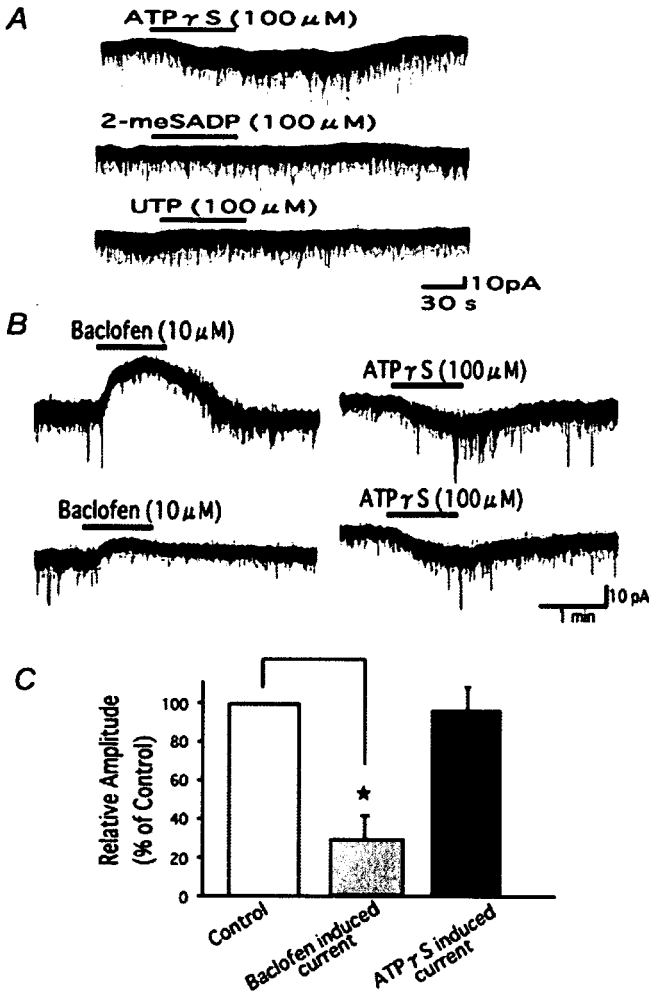

Figure 5. The ATPγS-induced inward current was not mediated by P2Y receptors

A, ATPγS (100 μM, upper trace) produced an inward current, while P2Y agonists, 2meSATP (100 μM, middle trace) or UTP (100 μM, lower trace) did not cause any inward current in the same lamina V neurones. *B*, the baclofen- and ATPγS-induced currents were recorded with the pipette solution containing GDPβS. Both baclofen and ATPγS affected the holding currents just after establishing whole-cell configuration in the same lamina V neurones (upper traces). When baclofen or ATPγS was again applied 1 h after establishing whole-cell configuration, the peak amplitude of the baclofen-induced outward current was clearly inhibited, while the ATPγS-induced inward current did not change (lower traces). *C*, a summary of the relative amplitude of the baclofen- and ATPγS-induced currents 1 h after establishing whole-cell configuration by the addition of GDPβS into the pipette solution. Under the same conditions as for *B*, the baclofen-induced outward current was significantly suppressed when baclofen was applied 1 h later (*$P < 0.05$). Error bars S.E.M.

Effects of P2X receptor agonist and antagonists

To clarify which subtype of P2X receptors is involved in the ATPγS-induced inward current, the effect of P2X receptor agonist and antagonists was examined. The bath application of $\alpha\beta$meATP (100 μM), an agonist for $P2X_1$, $P2X_3$, $P2X_{2/3}$, $P2X_{1/5}$ and $P2X_{4/6}$ receptors, did not induce any inward current in any of 28 lamina V neurones tested (Fig. 6*A* and *C*), although glutamatergic mEPSC frequency significantly increased in 17 out of 28 lamina V neurones (Fig. 6*A* and *D*). In addition, the effects of the P2X receptors antagonists, PPADS and TNP-ATP on the ATPγS-induced inward currents were examined. In the presence of PPADS (10 μM), the average amplitude of the ATPγS-induced inward current was −1.3 ± 0.2 pA, and it significantly decreased to 15 ± 4% of that in the absence of PPADS in the same lamina V neurones examined ($n = 7$, Fig. 6*B* and *C*). On the other hand, the average amplitude of the ATPγS-induced inward currents was −11.7 ± 1.6 pA in the presence of TNP-ATP (1 μM), which was not substantially different from that in the absence of TNP-ATP in the same neurones recorded (−11.0 ± 1.7 pA, $n = 7$, Fig. 6*B* and *C*). We further examined which subtype of P2X receptors is involved in the ATPγS-mediated increase in sEPSC frequency in lamina V neurones. The bath application of ATPγS (100 μM) significantly increased the frequency of glutamatergic EPSCs (203 ± 38% of the control, $n = 7$, Fig. 6*D*). The ATPγS-induced increase in sEPSC frequency was completely blocked by 10 μM PPADS (96 ± 10% of the control, $n = 7$), but it was not significantly affected by 1 μM TNP-ATP (182 ± 27% of the control, $n = 7$, Fig. 6*D*).

Developmental changes in P2X receptors in DDH neurones

To examine whether or not a developmental change in the P2X receptors existed in the lamina V neurones, whole-cell patch-clamp recordings were performed from lamina V neurones of P16–19 spinal cord slices. Interestingly, the bath application of ATPγS (100 μM) produced a clear inward current in all 11 lamina V neurones recorded at a holding potential of −70 mV (Fig. 7*B* and *C*). The average amplitude of the peak currents induced by ATPγS (100 μM) was −22.6 ± 4.2 pA ($n = 11$), which was significantly larger than that of P9–12 (Fig. 7*D*). In 10 out of these 11 neurones, the ATPγS-induced inward current was accompanied by a significant increase in the frequency of glutamatergic sEPSCs. The average increase in the sEPSC frequency by ATPγS (100 μM) was 318 ± 45.7% of the control

($n = 11$). On the other hand, $\alpha\beta$meATP (100 μM) did not affect the membrane current, but significantly increased glutamatergic sEPSC frequency in all seven lamina V neurones in which ATPγS produced an inward current (data not shown). These results suggest that a larger population of lamina V neurones elicited not only postsynaptic but also presynaptic P2X receptor-mediated actions in the later developmental days.

Discussion

In this study, we show that the distinct subtypes of P2X receptors are functionally expressed in both the post- and presynaptic sites of DDH neurones. Activation of the postsynaptic P2X receptor directly depolarizes the majority of lamina V neurones in spinal cord slices, in addition to our previous finding of presynaptic P2X receptor-mediated enhancement of glutamate release onto lamina V neurones (Nakatsuka & Gu, 2001; Nakatsuka *et al.* 2002, 2003). Furthermore, both the P2X receptor-mediated post- and presynaptic responses in the lamina V neurones were significantly greater in P16–19 than in P9–12, thus indicating that there might be a progressive expression of P2X receptors during maturation.

Expression of P2X receptors in DDH neurones

It has been demonstrated that all *P2X* mRNAs except $P2X_3$ are distributed in the DH (Collo *et al.* 1996). $P2X_2$, $P2X_4$, and $P2X_6$ mRNAs were strongly expressed in the SDH.

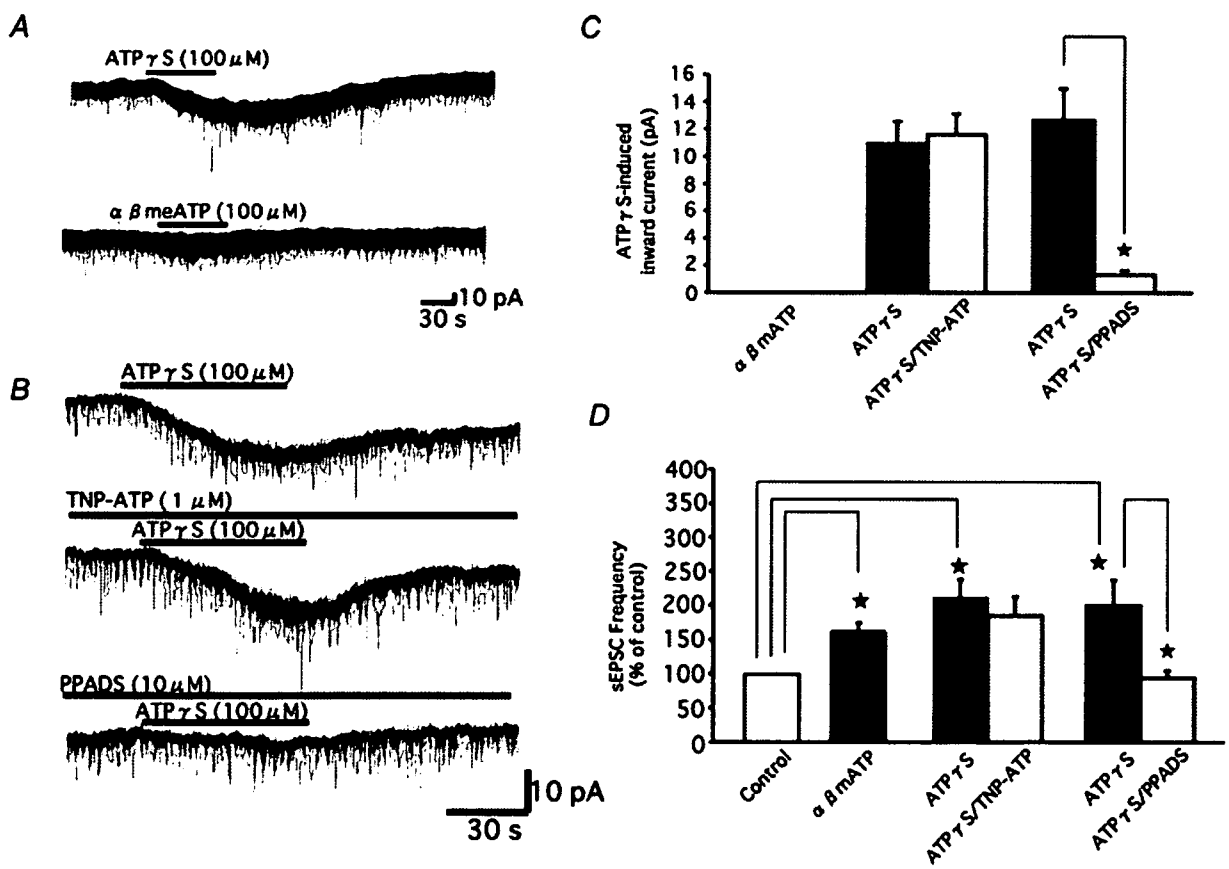

Figure 6. Effect of P2X agonist and antagonists
A, ATPγS (100 μM) induced an inward current (upper trace), while $\alpha\beta$meATP (100 μM), a P2X receptor agonist, did not cause any inward current in the same lamina V neurones (lower trace). *B*, TNP-ATP (1 μM), a P2X receptor antagonist, did not affect the ATPγS-induced inward current (middle trace). On the other hand, in the presence of PPADS (10 μM), the ATPγS-induced inward current was completely abolished in the same neurons (lower trace). *C*, a summary of the averaged amplitude of the inward currents by $\alpha\beta$meATP (100 μM), ATPγS (100 μM), ATPγS (100 μM) in the presence of TNP-ATP (1 μM), and ATPγS (100 μM) in the presence of PPADS (10 μM). The ATPγS-induced inward currents in the presence of PPADS were significantly smaller than those in the absence of PPADS (*$P < 0.05$). *D*, a summary of the relative sEPSC frequency before (control) and during the application of $\alpha\beta$meATP (100 μM), ATPγS (100 μM), ATPγS (100 μM) in the presence of TNP-ATP (1 μM), and ATPγS (100 μM) in the presence of PPADS (10 μM). Both $\alpha\beta$meATP and ATPγS significantly increased sEPSC frequency (*$P < 0.05$). The ATPγS-induced increase in sEPSC frequency was not significantly inhibited by TNP-ATP, but was markedly suppressed by PPADS (*$P < 0.05$). Error bars S.E.M.

Consistently, several electrophysiological studies have also described the direct action of ATP or its agonists on postsynaptic P2X receptors in SDH neurones. Jahr & Jessell (1983) first demonstrated that pressure application of ATP produced a rapid and marked depolarization in 27% of cultured SDH neurones. The ATP-induced inward current was reproduced by ATPγS, but not by P2Y receptor agonists in 38% of cultured SDH neurones (Hugel & Schlichter, 2000). Furthermore, in a small population (<5%) of acutely dissociated SDH neurones from P7–12 rats, intracellular Ca^{2+} concentration was significantly elevated by ATP (100 μM), but not by α,βmeATP (Bardoni *et al.* 1997). ATP also generated an inward current in 24% of the mechanically dissociated lamina II neurones from P10–P14 rats (Rhee *et al.* 2000). In hamster spinal cord slices (P21–28), high dose of ATP or ATPγS produced an inward current in approximately half of lamina II neurones (Li & Perl, 1995). However, there has been no report concerning postsynaptic P2X receptor-mediated actions in DDH neurones. In the present study, the bath application of ATPγS induced an inward current in the majority of lamina V neurones. The finding of no effect of TTX on the ATPγS-induced inward current suggests that ATPγS acts directly on the lamina V neurones, but not through an activation of interneurones. To eliminate the possibility of the involvement of P2Y receptors in the ATPγS-induced inward current, the effects of P2Y receptor agonists on synaptic transmission were examined in lamina V neurones. UTP, UDP, and 2meSADP, did not mimic the ATPγS-induced inward current. In addition, the ATPγS-induced inward current was not affected by the addition of GDPβS into the pipette solution. These findings suggested that ATPγS-induced inward current in lamina V neurones is mediated by ionotropic P2X, but not by metabotropic P2Y receptors. Consistent with the previous observations of functional P2X receptors in heterologous expression systems (Khakh *et al.* 2001; North, 2002), the reversal potential of the ATPγS-induced current in the present study was close to 0 mV, a value that was compatible with the activation of a non-selective cation conductance. As well as lamina V neurones, the ATP-induced inward current has been shown to be postsynaptically activated by ionotropic P2X, but not by metabotropic P2Y receptors in a subpopulation of SDH neurones (Bardoni *et al.* 1997; Hugel & Schlichter, 2000; Rhee *et al.* 2000).

ATPγS also significantly increased glutamatergic mEPSC frequency in 77% of lamina V neurones. This effect was similar to our previous findings of presynaptic P2X receptor-mediated enhancement of glutamate release onto lamina V neurones (Nakatsuka & Gu, 2001; Nakatsuka *et al.* 2002; Nakatsuka *et al.* 2003). Compared with ATPγS (77%), $\alpha\beta$meATP increased glutamatergic mEPSC frequency in a smaller population of lamina V neurones (61%). This result may be explained by the different sensitivities between the P2X receptor agonists, ATPγS and $\alpha\beta$meATP. However, we cannot conclusively rule out the possibility that ATPγS might activate P2X receptors in a subset of glutamatergic interneurones, because spinal DH neurones are directly excited by ATPγS, but not by $\alpha\beta$meATP (Bardoni *et al.* 1997; Nakatsuka & Gu, 2001). There is no reported evidence regarding this

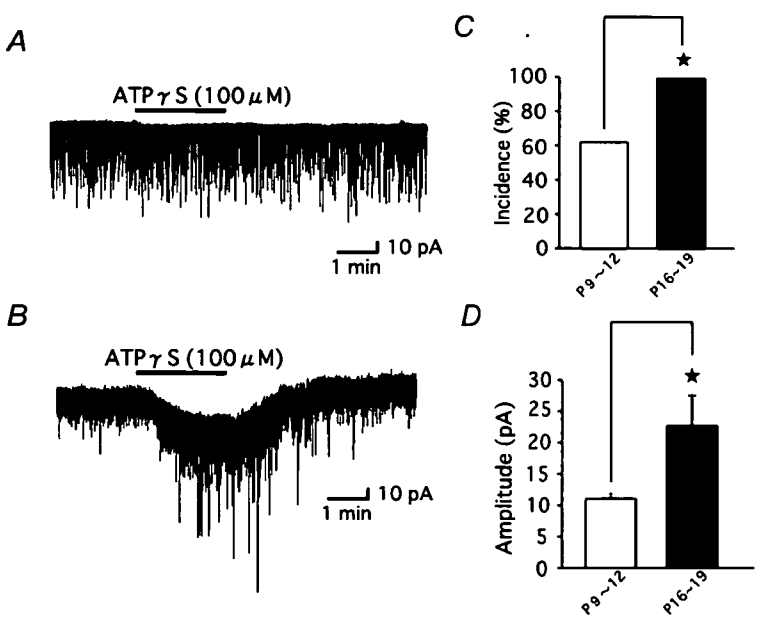

Figure 7. Developmental change of postsynaptic P2X receptors
A, ATPγS (100 μM) did not produce any membrane current in a P9–12 lamina V neurone. *B*, ATPγS (100 μM) induced a clear inward current in a P16–19 lamina V neurone. In contrast to P9–12 lamina V neurones, the ATPγS-induced inward current was observed in all P16–19 lamina V neurones examined. *C*, a summary of the incidence of the ATPγS-induced inward currents in P9–12 and P16–19 lamina V neurones. The population of P16–19 lamina V neurones which exhibited the inward current was significantly larger than that of P9–12 lamina V neurones (*$P < 0.05$). *D*, a summary of the averaged amplitude of the ATPγS-induced inward currents in P9–12 and P16–19 lamina V neurones at these stages. The average amplitude of the ATPγS-induced inward currents in P16–19 was significantly larger than that in P9–12 (*$P < 0.05$). Error bars S.E.M.

interesting issue. As a result, further investigations will be required to address whether functional P2X receptors are expressed in spinal glutamatergic interneurones.

Pharmachological property of postsynaptic P2X receptors

The ATPγS-induced inward current was accompanied by a significant increase in the frequency of glutamatergic mEPSCs in the majority of lamina V neurones. On the other hand, $\alpha\beta$meATP significantly increased glutamatergic mEPSC frequency, but it did not produce any inward currents in lamina V neurones. These results suggested that a subtype of postsynaptic P2X receptors is different from that of presynaptic P2X receptors. Due to a lack of good selective agonists and antagonists for each subtype of P2X receptors, it is hard to pharmacologically distinguish post- and presynaptic P2X receptors in lamina V neurones. Seven P2X receptor subunits have been identified and cloned (North & Surprenant, 2000). To date, six homomeric ($P2X_{1-5}$, $P2X_7$) and four heteromeric ($P2X_{1/5}$, $P2X_{2/3}$, $P2X_{2/6}$, $P2X_{4/6}$) P2X receptors have been characterized in heterologous expression systems (Khakh *et al.* 2001). ATPγS is a non-hydrolysable ATP analogue and a common agonist for all P2X receptors. On the other hand, $\alpha\beta$meATP selectively activates $P2X_1$, $P2X_3$, $P2X_{1/5}$, $P2X_{2/6}$ and $P2X_{4/6}$ receptors (Khakh *et al.* 2001). PPADS (10 μM) inhibits almost all P2X receptors except $P2X_4$ and $P2X_6$, although it is unknown whether the $P2X_{2/6}$ receptor is sensitive to PPADS (Khakh *et al.* 2001). TNP-ATP (1 μM) is an antagonist for $P2X_1$, $P2X_2$, $P2X_3$, $P2X_{2/3}$ and $P2X_{1/5}$, but it remains unknown whether $P2X_5$, $P2X_6$, $P2X_{2/6}$, and $P2X_{4/6}$ receptors are sensitive to TNP-ATP (Virginio *et al.* 1998; Surprenant *et al.* 2000; Khakh *et al.* 2001). In the present study, the ATPγS-induced inward current in DDH neurones was not reproduced by $\alpha\beta$meATP (100 μM), and was blocked by PPADS (10 μM) but not by TNP-ATP (1 μM). The pharmacological profile of postsynaptic P2X receptors in DDH neurones may be consistent with the involvement of $P2X_5$ and/or $P2X_{2/6}$ receptors. Consistent with these electrophysiological findings, *in situ* hybridization studies have shown that *P2X*$_2$, *P2X*$_5$, and *P2X*$_6$ mRNAs are expressed in the DDH (Collo *et al.* 1996). However, the involvement of $P2X_2$ or $P2X_4$ receptors could not be excluded in the present study, because $P2X_2$ and $P2X_4$ receptors are relatively insensitive to TNP-ATP (Virginio *et al.* 1998). So far, few tools have been developed to discriminate P2X receptors on naïve neurones.

Developmental changes of P2X receptors

The circuitry in the central nervous system might be altered by somatosensory inputs in early life (Anand, 2000; Peters *et al.* 2005). In addition, recent studies into the development of excitatory and inhibitory synaptic transmission have provided that nociceptive circuits in the spinal DH are organized and strengthened during the first postnatal weeks (Fitzgerald, 2005). It has been demonstrated that the presynaptic P2X receptor subtype in SDH changes during postnatal development (Jang *et al.* 2001). Although $\alpha\beta$meATP did not elicit any presynaptic or postsynaptic effects in mechanically dissociated P10–13 lamina II neurones, $\alpha\beta$meATP-sensitive P2X receptors were functionally expressed on the glycinergic presynaptic nerve terminals innervated onto P16–18 lamina II neurones. However, it remains unclear whether the expression of post- or presynaptic P2X receptors in DDH neurones can be altered during postnatal development. In the present study, we showed that ATPγS induced an inward current in 61% of P9–12 lamina V neurones and all P16–19 lamina V neurones. Interestingly, the average amplitude of the peak currents induced by ATPγS in P16–19 lamina V neurones was significantly larger than that in P9–12 lamina V neurones. In addition, ATPγS increased the mEPSC frequency in 77% of P9–12 lamina V neurones and 91% of P16–19 lamina V neurones. $\alpha\beta$meATP also increased the mEPSC frequency in 61% of P9–12 lamina V neurones and all P16–19 lamina V neurones. These results suggested that post- and presynaptic P2X receptors are therefore expressed in larger populations of lamina V neurones in later development. As a result, purinergic signalling in the DDH may become more common and important with the postnatal development.

Functional implications

DDH neurones participate in the processing of somatosensory information, including nociceptive inputs, and relay the information to supraspinal structures (Willis & Coggeshall, 1991). DDH neurones may generate prolonged afterdischarges in response to the nociceptive information (Woolf & King, 1987; De Koninck & Henry, 1991), and the hyperactivity of DDH neurones is believed to be associated with the development of pathological pain sensations, including neuropathic pain or inflammatory pain. The present study provides evidence that extracellular ATP could elicit two different actions in facilitating neuronal excitability through distinct post- and presynaptic P2X receptors in the DDH. Although the original source of endogenous ATP is unknown at present, ATP could be released in the central nervous system as a consequence of neuronal hyperactivity (Khakh & Henderson, 1998; Khakh *et al.* 2003; Koizumi *et al.* 2003). As a result, the activation of post- and/or presynaptic P2X receptors in DDH neurones may therefore contribute to a variety of pain sensations.

References

Anand KJ (2000). Effects of perinatal pain and stress. *Prog Brain Res* **122**, 117–129.

Bardoni R, Goldstein PA, Lee CJ, Gu JG & MacDermott AB (1997). ATP P2X receptors mediate fast synaptic transmission in the dorsal horn of the rat spinal cord. *J Neurosci* **17**, 5297–5304.

Burnstock G & Wood JN (1996). Purinergic receptors: their role in nociception and primary afferent neurotransmission. *Curr Opin Neurobiol* **6**, 526–532.

Chen M & Gu JG (2005). A P2X receptor-mediated nociceptive afferent pathway to lamina I of the spinal cord. *Mol Pain* **1**, 4.

Chizh BA & Illes P (2001). P2X receptors and nociception. *Pharmacol Rev* **53**, 553–568.

Collo G, North RA, Kawashima E, Merlo-Pich E, Neidhart S, Surprenant A & Buell G (1996). Cloning of P2X5 and P2X6 receptors and the distribution and properties of an extended family of ATP-gated ion channels. *J Neurosci* **16**, 2495–2507.

De Koninck Y & Henry JL (1991). Substance P-mediated slow excitatory postsynaptic potential elicited in dorsal horn neurons *in vivo* by noxious stimulation. *Proc Natl Acad Sci U S A* **88**, 11344–11348.

Fitzgerald M (2005). The development of nociceptive circuits. *Nat Rev Neurosci* **6**, 507–520.

Guo A, Vulchanova L, Wang J, Li X & Elde R (1999). Immunocytochemical localization of the vanilloid receptor 1 (VR1): relationship to neuropeptides, the P2X3 purinoceptor and IB4 binding sites. *Eur J Neurosci* **11**, 946–958.

Hamilton SG & McMahon SB (2000). ATP as a peripheral mediator of pain. *J Auton Nerv Syst* **81**, 187–194.

Hugel S & Schlichter R (2000). Presynaptic P2X receptors facilitate inhibitory GABAergic transmission between cultured rat spinal cord dorsal horn neurons. *J Neurosci* **20**, 2121–2130.

Jahr CE & Jessell TM (1983). ATP excites a subpopulation of rat dorsal horn neurones. *Nature* **304**, 730–733.

Jang IS, Rhee JS, Kubota H, Akaike N & Akaike N (2001). Developmental changes in P2X purinoceptors on glycinergic presynaptic nerve terminals projecting to rat substantia gelatinosa neurones. *J Physiol* **536**, 505–519.

Kennedy C, Assis TS, Currie AJ & Rowan EG (2003). Crossing the pain barrier: P2 receptors as targets for novel analgesics. *J Physiol* **553**, 683–694.

Khakh BS (2001). Molecular physiology of P2X receptors and ATP signalling at synapses. *Nat Rev Neurosci* **2**, 165–174.

Khakh BS, Burnstock G, Kennedy C, King BF, North RA, Seguela P, Voigt M & Humphrey PP (2001). International union of pharmacology. XXIV. Current status of the nomenclature and properties of P2X receptors and their subunits. *Pharmacol Rev* **53**, 107–118.

Khakh BS, Gittermann D, Cockayne DA & Jones A (2003). ATP modulation of excitatory synapses onto interneurons. *J Neurosci* **23**, 7426–7437.

Khakh BS & Henderson G (1998). ATP receptor-mediated enhancement of fast excitatory neurotransmitter release in the brain. *Mol Pharmacol* **54**, 372–378.

Koizumi S, Fujishita K, Tsuda M, Shigemoto-Mogami Y & Inoue K (2003). Dynamic inhibition of excitatory synaptic transmission by astrocyte-derived ATP in hippocampal cultures. *Proc Natl Acad Sci U S A* **100**, 11023–11028.

Li P, Calejesan AA & Zhuo M (1998). ATP P2X receptors and sensory synaptic transmission between primary afferent fibers and spinal dorsal horn neurons in rats. *J Neurophysiol* **80**, 3356–3360.

Li J & Perl ER (1995). ATP modulation of synaptic transmission in the spinal substantia gelatinosa. *J Neurosci* **15**, 3357–3365.

Liu XJ & Salter MW (2005). Purines and pain mechanisms: recent developments. *Curr Opin Invest Drugs* **6**, 65–75.

Mao J, Price DD, Coghill RC, Mayer DJ & Hayes RL (1992). Spatial patterns of spinal cord [14C]-2-deoxyglucose metabolic activity in a rat model of painful peripheral mononeuropathy. *Pain* **50**, 89–100.

Nakatsuka T, Furue H, Yoshimura M & Gu JG (2002). Activation of central terminal vanilloid receptor-1 receptors and $\alpha\beta$-methylene-ATP-sensitive P2X receptors reveals a converged synaptic activity onto the deep dorsal horn neurons of the spinal cord. *J Neurosci* **22**, 1228–1237.

Nakatsuka T & Gu JG (2001). ATP P2X receptor-mediated enhancement of glutamate release and evoked EPSCs in dorsal horn neurons of the rat spinal cord. *J Neurosci* **21**, 6522–6531.

Nakatsuka T, Park JS, Kumamoto E, Tamaki T & Yoshimura M (1999). Plastic changes in sensory inputs to rat substantia gelatinosa neurons following peripheral inflammation. *Pain* **82**, 39–47.

Nakatsuka T, Tsuzuki K, Ling JX, Sonobe H & Gu JG (2003). Distinct roles of P2X receptors in modulating glutamate release at different primary sensory synapses in rat spinal cord. *J Neurophysiol* **89**, 3243–3252.

North RA (2002). Molecular physiology of P2X receptors. *Physiol Rev* **82**, 1013–1067.

North RA & Surprenant A (2000). Pharmacology of cloned P2X receptors. *Annu Rev Pharmacol Toxicol* **40**, 563–580.

Peters JW, Schouw R, Anand KJ, van Dijk M, Duivenvoorden HJ & Tibboel D (2005). Does neonatal surgery lead to increased pain sensitivity in later childhood? *Pain* **114**, 444–454.

Rhee JS, Wang ZM, Nabekura J, Inoue K & Akaike N (2000). ATP facilitates spontaneous glycinergic IPSC frequency at dissociated rat dorsal horn interneuron synapses. *J Physiol* **524**, 471–483.

Surprenant A, Schneider DA, Wilson HL, Galligan JJ & North RA (2000). Functional properties of heteromeric $P2X_{1/5}$ receptors expressed in HEK cells and excitatory junction potentials in guinea-pig submucosal arterioles. *J Auton Nerv Syst* **81**, 249–263.

Virginio C, Robertson G, Surprenant A & North RA (1998). Trinitrophenyl-substituted nucleotides are potent antagonists selective for $P2X_1$, $P2X_3$, and heteromeric $P2X_{2/3}$ receptors. *Mol Pharmacol* **53**, 969–973.

von Kügelgen I & Wetter A (2000). Molecular pharmacology of P2Y-receptors. *Naunyn Schmiedebergs Arch Pharmacol* **362**, 310–323.

Vulchanova L, Riedl MS, Shuster SJ, Buell G, Surprenant A, North RA & Elde R (1997). Immunohistochemical study of the $P2X_2$ and $P2X_3$ receptor subunits in rat and monkey sensory neurons and their central terminals. *Neuropharmacology* **36**, 1229–1242.

Willis WD & Coggeshall RE (1991). *Sensory Mechanisms of the Spinal Cord*. Plenum, New York.

Woolf CJ & King AE (1987). Physiology and morphology of multireceptive neurons with C-afferent fiber inputs in the deep dorsal horn of the rat lumbar spinal cord. *J Neurophysiol* **58**, 460–479.

Acknowledgements

We thank Ms. H. Mizuguchi-Takase for the histological support. This work was supported by The Japanese Health Sciences Foundation (No. KH21006) to T.N., and Grants-in-Aid for Scientific Research from the Ministry of Education, Science, Sports and Culture of Japan (No. 17700370) to T.N. and (Nos 16650089 and 17200027) to M.Y.

0026-895X/06/7001-319–328$20.00
MOLECULAR PHARMACOLOGY
Copyright © 2006 The American Society for Pharmacology and Experimental Therapeutics
Mol Pharmacol 70:319–328, 2006

Vol. 70, No. 1
20511/3124430
Printed in U.S.A.

Retinoic Acids Increase $P2X_2$ Receptor Expression through the 5′-Flanking Region of *P2rx2* Gene in Rat Phaeochromocytoma PC-12 Cells

Hidetoshi Tozaki-Saitoh, Schuichi Koizumi, Yoji Sato, Makoto Tsuda, Taku Nagao, and Kazuhide Inoue

Divisions of Pharmacology (H.T.-S., S.K.) and Cellular and Gene Therapy Products (Y.S.), National Institute of Health Sciences, Tokyo, Japan; National Institute of Health Sciences, Tokyo, Japan (T.N.); and Department of Molecular and System Pharmacology, Graduate School of Pharmaceutical Sciences, Kyushu University, Fukuoka, Japan (H.T.-S., M.T., K.I.)

Received November 1, 2005; accepted April 25, 2006

ABSTRACT

The $P2X_2$ receptor is a subtype of ionotropic ATP receptor and plays a significant role in regulating fast synaptic transmission in the nervous system. Because the expression level of the $P2X_2$ receptor is known to determine its channel properties and functional interactions with other neurotransmitter channels, elucidating the mechanisms underlying the regulation of $P2X_2$ receptor expression in neuronal cells is important. Here, we identified three motifs that correspond to the retinoic acid response element in the 5′-flanking region of the rat $P2X_2$ gene. In rat pheochromocytoma PC-12 cells, treatment with 9-*cis*-retinoic acid as well as all-*trans*-retinoic acid significantly increased the mRNA and protein level of $P2X_2$ receptor. In addition, in PC-12 cells transiently transfected with a luciferase reporter gene driven by the promoter region of the rat $P2X_2$ gene, both 9-*cis*-retinoic acid and all-*trans*-retinoic acid increased the luciferase activity, whereas their effects were diminished by truncation of the retinoic acid response elements in the promoter. Furthermore, 9-*cis*-retinoic acid enhanced the ATP-evoked whole cell currents and intracellular Ca^{2+}- and ATP-evoked dopamine release, indicating the up-regulation of functional $P2X_2$ receptors on the plasma membrane. These results provide the molecular mechanism underlying the transcriptional regulation of $P2X_2$ receptors and suggest that retinoid is an important factor in regulating $P2X_2$ receptors in the nervous system.

P2X receptors, of which seven subtypes ($P2X_1$–$P2X_7$) have so far been cloned, are a family of ligand-gated cation channels activated by extracellular ATP and are widely expressed in the peripheral and central nervous system (North, 2002; Illes and Alexandre Ribeiro, 2004). A growing body of evidence indicates that P2X receptors expressed in neurons play important roles in mediating (Galligan and Bertrand, 1994), facilitating presynaptically (Khakh et al., 2003; Shigetomi and Kato, 2004), and modulating postsynaptically fast excitatory and inhibitory synaptic transmission (Wang et al., 2004). It remains unclear which P2X receptor subtypes are the main targets for ATP at synapses, but several lines of evidence have suggested the $P2X_2$ receptor as a candidate. In several regions of the nervous system, neurons express functional $P2X_2$ receptors (North, 2002; Illes and Alexandre Ribeiro, 2004) as well as both the mRNA and protein of $P2X_2$ receptors (Kanjhan et al., 1999). An electron microscopic study has shown that $P2X_2$ receptors are localized at the postsynaptic membrane in the cerebellum and the CA1 region of the hippocampus (Rubio and Soto, 2001). In addition, it has been reported that $P2X_2$ receptors are abundant in the biochemically fractionated presynaptic active zone in the hippocampus (Rodrigues et al., 2005). A recent study has shown that ATP facilitates excitatory glutamate transmission onto stratum radiatum interneurons, a population of the ATP-

This work was partly supported by The National Institute of Biomedical Innovation (Medical Frontier Project; MF-16), The Health Science Foundation in Japan, and a grant-in-aid for scientific research from the Ministry of Education, Science, Sports and Culture.

Article, publication date, and citation information can be found at http://molpharm.aspetjournals.org.

doi:10.1124/mol.105.020511.

ABBREVIATIONS: RARE, retinoic acid response element; RAR, retinoic acid receptor; RXR, retinoid X receptor; DA, dopamine; VDCC, voltage-dependent calcium channel; RA, retinoic acid; RT-PCR, reverse transcriptase polymerase chain reaction; bp, base pair(s); PCR, polymerase chain reaction; TESS, transcription element search system; RACE, rapid amplification of cDNA ends; $P2X_2R$, $P2X_2$ receptor; GAPDH, glyceraldehyde-3-phosphate dehydrogenase; GFP, green fluorescent protein; BSS, balanced salt solution; PCA, perchloric acid; AP, adaptor protein; atRA, all-*trans*-retinoic acid; PPADS, pyridoxal phosphate-6-azophenyl-2′4′-disulfonic acid; U-73122, 1-[6-[[17β-methoxyestra-1,3,5(10)-trien-17-yl]amino]hexyl]-1*H*-pyrrole-2,5-dione; DR, direct repeat; ANOVA, analysis of variance.

responding neurons that is markedly reduced in hippocampus slices from $P2X_2$-deficient mice (Khakh et al., 2003). These results indicate that in several regions $P2X_2$ receptors localized at pre- and/or postsynapses regulate fast synaptic transmission. Furthermore, $P2X_2$ receptors are associated directly with other neurotransmitter channels such as nicotinic acetylcholine receptors, 5-hydroxytryptamine receptors or $GABA_A$ receptors, and activation of both receptors produces nonadditive cross-inhibitory responses (Khakh et al., 2000; Boue-Grabot et al., 2003). It is noteworthy that the functional interaction of $P2X_2$ receptors with other channels is decreased at lower densities of channel expression (Khakh et al., 2000), suggesting that their expression levels affect cellular events resulting from activation of $P2X_2$ receptors at synapses. In addition, the expression level of $P2X_2$ receptors also changes their channel properties (Fujiwara and Kubo, 2004). Moreover, an increase in the expression of $P2X_2$ receptors in neuronal cells has been implicated in the development of several pathological states such as brain ischemia and chronic pain (Xu and Huang, 2002; Cavaliere et al., 2003). Therefore, to understand the physiological and pathological roles of $P2X_2$ receptors in the functioning of the nervous system, it is of particular importance to determine how the expression of $P2X_2$ receptors is regulated in neuronal cells.

In the present study, we cloned the 5′-flanking region of the rat $P2X_2$ gene (*P2rx2*) and identified three sites corresponding to a motif of retinoic acid response element (RARE). RARE is a binding site of nuclear receptors, including retinoic acid receptor (RAR) and retinoid X receptor (RXR), and is required for the gene expression induced by retinoids (Chambon, 1996). We further found that retinoids increase both the mRNA and protein expression of the $P2X_2$ receptor and enhance release of the neurotransmitter dopamine (DA) evoked by ATP through activating $P2X_2$ receptors from rat pheochromocytoma PC-12 cells, a neuronal model (Shafer and Atchison, 1991). Therefore, these results suggest that retinoids are regulators of the expression of $P2X_2$ receptors in neuronal cells in the nervous system.

Materials and Methods

PC-12 Cells. PC-12 cells (passage 55–70) were cultured according to Inoue and Kenimer (1988), and undifferentiated cells were used. Cells were cultured in Dulbecco's modified eagle's medium supplemented with 7.5% fetal bovine serum, 7.5% horse serum, and 4 mM L-glutamine. For reverse transcription-polymerase chain reaction (RT-PCR) and Western blot experiments, cells were plated on 60-mm collagen (Virtogen-100)-coated dishes for 2 days. For whole cell patch-clamp recording and intracellular calcium imaging, cells were plated on collagen-coated coverslips placed on the bottom of 35-mm polystyrene dishes. For the measurement of DA release, cells were plated on collagen-coated 35-mm polystyrene dishes.

Cloning of the $P2X_2$ Upstream Region. Sequences for the 5′-flanking region of *P2rx2* were obtained from National Center for Biotechnology Information Rat Genome Resources. The genomic 2.5-kb upstream sequence of the putative Wistar rat *P2rx2* transcription starting site was targeted as $P2X_2$ mRNA (GenBank accession number NM_053656) upstream sequence. The following primers were designed for amplification of the 5′-flanking region of *P2rx2*: forward primer, GAACCTCGAGTGAGCCACAACCAGAACACT; reverse primer, GACAAGATCTATGGCCCAAGGAGCTCGGT. Genomic DNA extracted from the tail of a female Wistar rat was used for the polymerase chain reaction. Four individual reactions were carried out, and amplicons were inserted in a pGEM-T vector (Promega, Madison, WI) for sequencing. Each insert was sequenced, and the exact sequence was estimated by comparing the four sequences. The relative location of the cloned sequence is confirmed to be just upstream of the first exon of *P2rx2* without any intervening inserts. Using primers specific to the third exon of *P2rx2* and −164 position of the cloned sequence, approximately 750-bp single-band amplification was obtained by PCR. This amplicon included the sequence comprising the 5′ site of $P2X_2$ mRNA (RefSeq sequence NM_053656) exactly as published, and the sequence was determined to be the 5′-flanking region without any additional intervening sequence. The sequence data from the 5′-flanking region of *P2rx2* has been deposited in GenBank with the accession number AY749416. Putative sites for the transcription element were analyzed using Transcription Element Search System (TESS) site (http://www.cbil.upenn.edu/tess).

"Oligo-Capping" 5′ Rapid Amplification of cDNA Ends of $P2X_2$ mRNA. Modified rapid amplification of 5′ cDNA ends (5′ RACE) was performed according to oligo-capping method developed by Maruyama and Sugano (1994). Total RNA (5 μg) extracted from PC-12 cells was treated with 1 unit of bacterial alkaline phosphatase (Takara, Kyoto, Japan) in supplied buffer with 100 units of RNase inhibitor (Toyobo, Osaka, Japan) at 37°C for 30 min to hydrolyze the phosphate of truncated mRNA 5′ ends. After extraction with phenol/chloroform (1:1) twice, chloroform once, and ethanol precipitation, tobacco acid pyrophosphatase (20 units; Wako Pure Chemicals, Osaka, Japan) was reacted (37°C; 15 min) in kit supplied buffer with RNase inhibitor to remove the cap structure of complete mRNAs. After phenol/chloroform extraction and ethanol precipitation, ligation reaction was carried with T4 RNA ligase (Takara) and 0.5 μg of 5′-adapter RNA oligonucleotide to obtain the oligonucleotide composed by mRNAs attached with 5′-adapter RNA oligonucleotide at 5′ ends that originally had the cap structure. After unligated 5′-adapter oligonucleotide was removed by repeating ethanol precipitation with high salt concentration, reverse transcription reaction was performed using ReverTra Ace (Toyobo) with antisense primer of $P2X_2$ mRNA, which was designed from +531 of NM_053656, and PCR was carried out with obtained cDNAs and primers for adapter and $P2X_2$ mRNA sequence, which were designed to cross the border of exons 1 and 2. The reaction mixture was electrophoresed in agarose gel, and all of amplicon was gel extracted and restricted by XhoI, whose restriction site was designed in adapter sequence. The fragments were cloned into pcDNA3 vector which restricted by XhoI and EcoRV and sequenced. The adapter and primers sequences are as follows. The 5′-adapter RNA oligonucleotide was 5′-GUCUGAGCUCUCGAGAUAGA-3′; the primer for reverse transcription, 5′-GTTGTCAGAAGTTCCATCCTCCAC-3′; the primer for 5′-adapter, 5′-GTCTGAGCTCTCGAGATAGA-3′; and the reverse primer for target amplification, 5′-CGATGAAGACGTACCACACGAA-3′.

Real-Time Quantitative RT-PCR (TaqMan RT-PCR). Retinoids were dissolved in ethanol and added to the culture medium so that the ethanol represented 0.1% of the v/v concentration. Total cellular RNA was prepared using the RNeasy method from QIAGEN (Valencia, CA) according to the manufacturer's instructions and included an on-column DNase I digestion to minimize genomic DNA contamination. The TaqMan One-Step RT-PCR Master Mix Reagent kit (Applied Biosystems, Foster City, CA) was used with each custom designed, gene-specific primer/probe set to amplify and quantify each transcript of interest. Reactions (25 μl) contained 50 ng of total RNA, 200 nM forward and reverse primers, 100 nM TaqMan probe, and RNase Inhibitor Mix in the Master Mix solution. RT-PCR amplification and real-time detection were performed using an ABI PRISM 7700 sequence detection system (Applied Biosystems) for 30 min at 48°C (reverse transcription), 10 min at 95°C (AmpliTaq Gold activation), 38 cycles of denaturation (15 s at 95°C), and annealing/extension (60 s at 60°C). Data were analyzed using ABI Prism Sequence Detection Software, version 1.1. The following primers and probes were used. The TaqMan probe for $P2X_2R$ was 5′-5-carboxy-

fluorescein-CACTACTCCCAGGATCAGCCACCCA-5-carboxytetramethylrhodamine-3'; the forward primer for $P2X_2R$, 5'-CATATCCCTCCCCCACCTA-3'; and the reverse primer, 5'-GTTGGTCCTTCACCTGATGGA-3'. Sense and antisense primers and probes for GAPDH were obtained from Rodent GAPDH Control Reagents (Applied Biosystems).

Plasmids. The 5'-flanking region of *P2rx2* (described above) was inserted into multicloning sites of the pGL3-basic vector (termed pP2X2luc; Promega). The sequence between two KpnI sites (one site is in the multicloning site and other site is at the −1923 position) in the vector was restricted by KpnI (Takara) and ligated to construct a deletion mutant which lacks 501 bp of the 5' end in the pP2X2luc insert (Del-pP2X2luc). The P2X2-GFP vector was a kind gift from Dr. Murrell-Lagnado (Department of Pharmacology, Cambridge University, Cambridge, UK).

Transient Transfections and Luciferase Assays. Transient transfection was carried out with Superfect (QIAGEN) according to the manufacturer's protocol. Fifty percent confluent cells seeded on 48-well plates were transfected with reporter plasmid (pP2X2luc, Del-pP2X2luc, P2X2-GFP). The phRL-TK vector (Promega) was cotransfected to monitor the transfection efficiency. After 48 h incubation, the cells were lysed. Firefly and *Renilla reniformis* luciferase activity were measured by 1420 ARVOsx multilabel counter (PerkinElmer Wallac, Turku, Finland) using a dual-luciferase reporter assay system (Promega). The transfection efficiency was corrected by normalizing the firefly luciferase activity to the *R. reniformis* luciferase activity.

Western Blot of $P2X_2$ Receptor Protein. After treatment of the cells with 9-*cis*-retinoic acid (9-*cis*-RA) for 1 day, the cells were washed with phosphate-buffered saline(−) twice and lysed in buffer containing 10 mM Tris-HCl, pH 7.4, 150 mM NaCl, 10 mM EDTA, 5 mM EGTA, 0.5% mM Nonidet P-40, and 0.5% deoxycholate. The protein concentration was measured by bicinchoninic acid protein assay (Pierce Chemical, Rockford, IL). Proteins (10–30 μg/lane) were mixed with SDS sample buffer, loaded onto a 10% polyacrylamide gel, electrophoresed, and transferred onto a nitrocellulose membrane. The membrane was then blocked in 5% nonfat dry milk in Tris-buffered saline containing 0.1% Tween 20. The membrane was incubated with the anti-rabbit $P2X_2$ polyclonal antibody (1:200; Calbiochem, San Diego, CA) or β-actin (1:5000; Sigma-Aldrich, St. Louis, MO) overnight at 4°C, followed by incubation with the horseradish peroxidase-conjugated anti-rabbit antibody (1:2000; GE Healthcare, Little Chalfont, Buckinghamshire, UK). The blots were probed with an ECL Western blot detection system (GE Healthcare). Quantification of immunoreactive bands was performed by scanned image analysis on a computer.

Whole Cell Patch-Clamp Recording. The cells were placed in a recording chamber and continuously superfused at room temperature (22–24°C) in an extracellular solution containing 140 mM NaCl, 5.4 mM KCl, 1.8 mM $CaCl_2$, 1.0 mM $MgCl_2$, 11.1 mM D-glucose, and 10 mM HEPES; pH adjusted to 7.4 with NaOH. Patch pipettes were filled with an intracellular solution containing 150 mM CsCl, 10 mM HEPES, and 5 mM EGTA; pH adjusted to 7.3 with CsOH. With this solution, patch electrode resistances ranged between 5 and 8 MΩ. The whole cell patch-clamp was made, and cells were voltage-clamped at −60 mV. ATP was diluted with extracellular solution and applied to the patched cell by gravity from a tube (300-μm inner diameter) attached to an electrically controlled valve. Currents were recorded with an Axopatch 200-B amplifier (Molecular Devices, Sunnyvale, CA) and analyzed using pClamp5 software (Molecular Devices).

Measurement of DA Released from PC-12 Cells. Cells were plated on 35-mm dishes and washed twice with 1 ml of balanced salt solution (BSS) containing 150 mM NaCl, 5 mM KCl, 1.2 mM $CaCl_2$, 1.2 mM $MgCl_2$, 25 mM HEPES, and 10 mM D-glucose and then incubated for 1 h with 1 ml of BSS at room temperature. The cells were again washed with BSS and then stimulated by BSS with or without 30 μM ATP for 1 min. BSS was collected in 1.5-ml tubes loaded with 250 μl of 1 N perchloric acid (PCA), and 1 ml of 0.2 N PCA was added to the dishes and incubated for 2 h on ice. Both the collected PCA solutions were centrifuged, and then the supernatants were used for DA measurement. The amount of DA in the solution was measured using high-performance liquid chromatography combined with electrochemical detection.

Intracellular Calcium Imaging. The increase in $[Ca^{2+}]_i$ in single cells was measured by the fura-2 method with minor modifications. Cells were washed with BSS and incubated with 10 μM fura-2 acetoxymethyl ester at 37°C in BSS for 45 min. The coverslips were mounted on an inverted epifluorescence microscope (TMD-300; Nikon, Tokyo, Japan) equipped with a 75-W xenon lamp and band-pass filters of 340-nm wavelength for measurement of the Ca^{2+}-dependent signal (F_{340}) and 360-nm wavelength for measurement of the Ca^{2+}-independent signal (F_{360}).

Results

Homology Search for Transcription Factor Binding Sites in the 5'-Flanking Region of *P2rx2*. The *P2rx2* is located at rat chromosome 12 and has 11 exons between 5'- and 3'-untranslated region (National Center for Biotechnology Information Entrez GeneID 114115). $P2X_2$ mRNA sequence has been first determined by Brake et al. (1994). Of 11 splicing variants registered in GenBank database, only two variants are reported to express functional channel (*P2rx2*, NM_053656; *P2X 2b*, Y10473). The information of the 5'-flanking region of the rat *P2rx2* was obtained from National Center for Biotechnology Information Rat Genome Resources. In the *Rattus norvegicus* (Norway rat) chromosome 12 genomic contig from whole genome shotgun sequence (NW_047378), putative transcription start site of *P2rx2* is predicted by searching the sequence location of rat $P2X_2$ mRNA (NM_053656) using BLAST. Then, a 2524-bp fragment upstream of the Wistar rat *P2rx2* was cloned in the pGL3 vector. Whether the cloned sequence is located in the 5'-flanking region of *P2rx2* is confirmed by sequencing the 743-bp amplicon obtained by genome PCR using specific primers for the third exon of *P2rx2* and our cloned sequence. The homology between database sequence and the cloned sequence was more than 99.8% match. In the cloned sequence, we found three putative RAREs that conformed with a general canonical sequence in which two directly repeated hexanucleotide motifs [consensus (A/G)G(G/T)TCA] are separated by one (DR1: −2309/−2321), four (DR4: −2299/−2314), and five nucleotides (DR5: −2408/−2424) (Fig. 1). We used TESS to verify these sites and confirmed that they were predicted as RAREs. The sequence analysis using TESS also predicted the presence of many consensus sequences for various transcription factors in the cloned fragment such as simian virus 40 protein 1 (Sp-1), AP-1, AP-2, GATA-1, nuclear factor-κB, and cAMP response element-binding protein binding motifs. Sequence data from the 5'-flanking region of the Wistar rat *P2rx2* have been deposited in GenBank with the accession number AY749416. Furthermore using oligo-capping 5' RACE, we could obtain single sequence that encodes 5' region of $P2X_2$ mRNA, suggesting that transcription starting site of *P2rx2* in PC-12 cells is located in 27 bases upstream of RefSeq sequence (NM_053656). Consensus sequences of GC-box (GGGCGG) and initiator (YYANWYY), which are expected to form core promoter region, were found in −67 and −52 bp upstream of transcription starting site determined with oligo-capping 5' RACE.

$P2X_2$ mRNA Level Is Increased by Retinoids Treatment in PC-12 Cells. The presence of putative RAREs in the 5′-flanking region of the *P2rx2* indicated the possibility that retinoids may change the expression of $P2X_2$ receptors. We examined the level of the $P2X_2$ mRNA expression in PC-12 cells that had been treated with or without 9-*cis*-RA, an active form of an endogenous vitamin A derivative, using real-time quantitative RT-PCR analysis. We found that the $P2X_2$ mRNA in 9-*cis*-RA (100 nM)-treated PC-12 cells was markedly increased and the highest level was observed as early as 3 h later ($n = 4$; ***, $p < 0.001$), and the increase persisted for at least 12 h after the treatment with 9-*cis*-RA ($n = 4$; ***, $p < 0.001$) (Fig. 2A). The increase in the level of $P2X_2$ mRNA by 9-*cis*-RA was dose-dependent, and a significant increase was seen at 100 and 1000 nM 9-*cis*-RA (Fig. 2B).

9-*cis*-RA is known to be an activator of the nuclear receptors RXR and RAR (Aranda and Pascual, 2001). RXR can form as homodimers and as heterodimers with a number of other nuclear receptors such as RAR (Aranda and Pascual, 2001). To clarify the nuclear receptors involved in the increase in the level of $P2X_2$ mRNA, we used two ligands, all-*trans*-retinoic acid (atRA) (Aranda and Pascual, 2001) and PA024 (Takahashi et al., 2002), agonists preferentially of RAR and RXR, respectively. In this experiment, PC-12 cells were cultured in serum-free medium to detect only the effects of RAR and RXR agonists because serum contains large amounts of retinoids and binding protein (Mori, 1978). In this condition, a dose-dependent increase in the level of $P2X_2$ mRNA was also observed in cells treated with 9-*cis*-RA (Fig. 3) as in cells grown in medium with serum (Fig. 2). We treated PC-12 cells with atRA and found that the level of

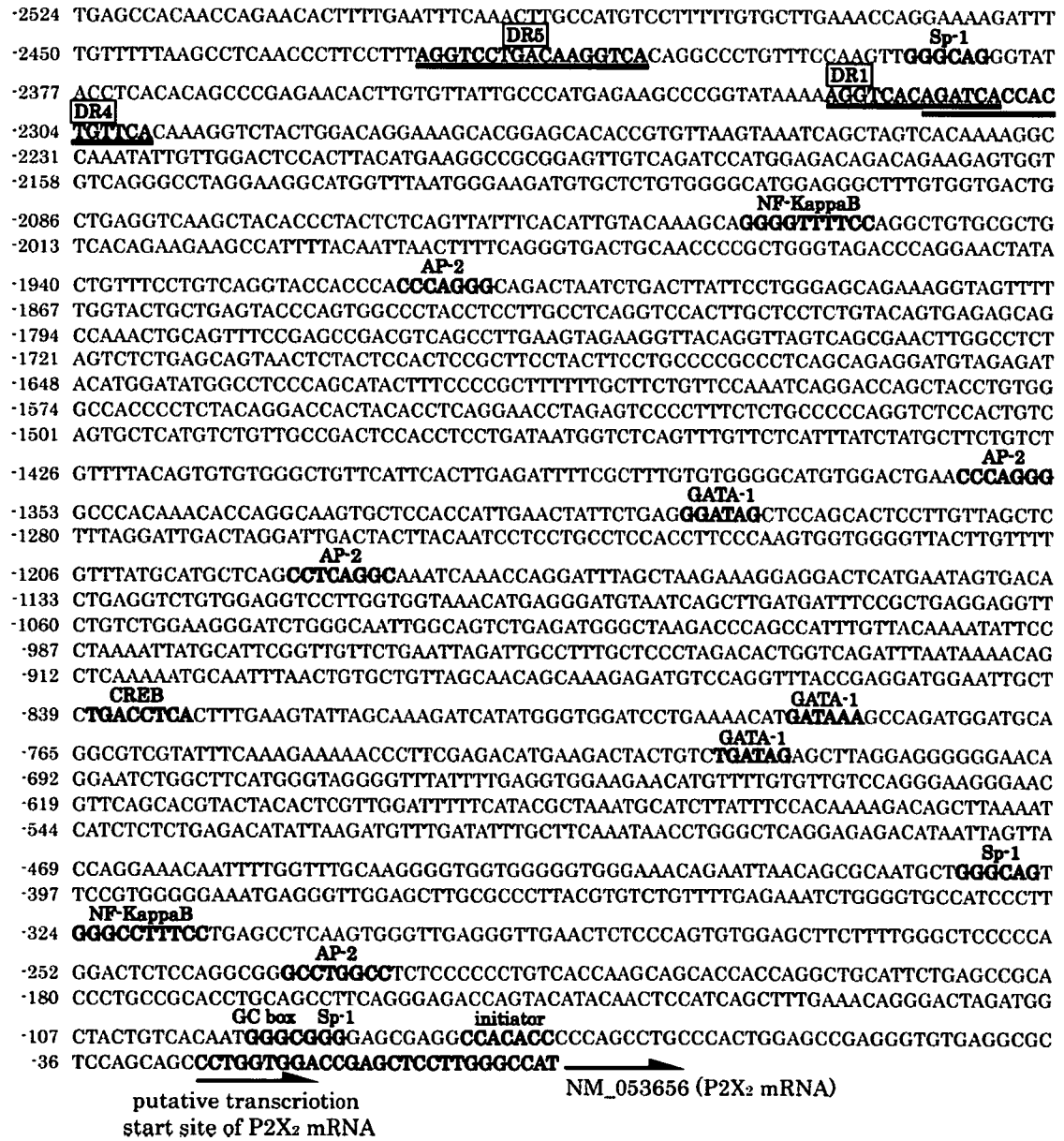

Fig. 1. Nucleotide sequence of the 5′-flanking region of the Wistar rat *P2rx2*. A 2524-base pair genomic sequence of 5′-flanking region of *P2rx2* was cloned and sequenced (GenBank accession no. AY749416) and analyzed to search for consensus motifs interacting with transcription factors using TESS. Predicted RAREs, sequences are underlined and indicated in bold. Other potential transcription binding sites predicted by TESS are indicated in bold. Arrows represent the location of $P2X_2$ mRNA sequences indicated by RefSeq sequence and 5′ RACE analysis.

$P2X_2$ mRNA was markedly increased. The increase was in a dose-dependent manner, and a significant increase was seen at the range of 10 to 1000 nM atRA (Fig. 3). By contrast, the preferential agonist of RXR, PA024 (1–100 nM), did not increase the level of $P2X_2$ mRNA. Because PC-12 cells undergo apoptotic cell death by serum deprivation (Batistatou and Greene, 1993), we maintained cells in serum-containing medium for other experiments.

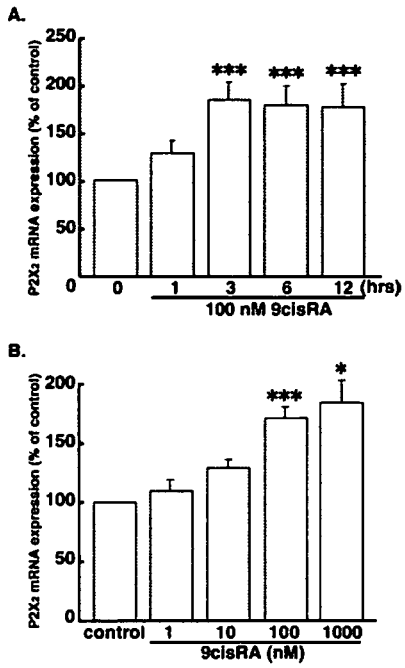

Fig. 2. Increase in the level of $P2X_2$ receptor mRNA by 9-*cis*-retinoic acid. PC-12 cells were treated with 100 nM 9-*cis*-RA for 1, 3, 6, and 12 h (A) or with different concentrations of 9-*cis*-RA (1–1000 nM) (B) followed by real-time RT-PCR analysis of $P2X_2$ and GAPDH mRNAs. $P2X_2$ mRNA levels were normalized by GAPDH mRNA levels, and each set of data represents the means ± S.E.M. of percentages of control from four individual experiments (***, $p < 0.001$; *, $p < 0.05$, multiple comparisons versus control group using Bonferroni t test after one-way ANOVA).

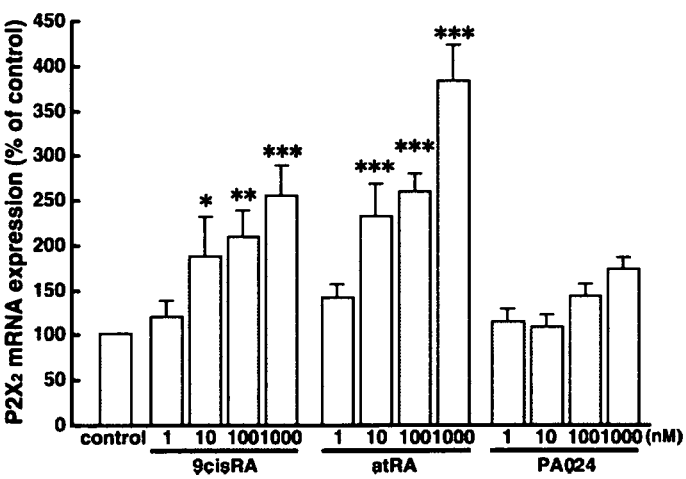

Fig. 3. Effects of selective RAR and RXR agonists on the level of $P2X_2$ receptor mRNA. PC-12 cells were treated with 9-*cis*-RA, atra, or PA024 at different concentrations for 3 h in serum-free condition followed by real-time RT-PCR analysis of $P2X_2$ and GAPDH mRNAs. $P2X_2$ mRNA levels were normalized by the GAPDH mRNA levels, and each set of data represents the means ± S.E.M. of the percentage over the value of the control group from four individual experiments (***, $p < 0.001$; **, $p < 0.01$; *, $p < 0.05$, multiple comparisons versus control group using Bonferroni t test after one-way ANOVA).

Retinoids Stimulate the Promoter Activity Driven by the 5′-Flanking Region of *P2rx2*. To determine whether 9-*cis*-RA increases $P2X_2$ mRNA at the transcriptional level, we examined the transcriptional activity of the 5′-flanking region of *P2rx2* (Fig. 4) using a dual-luciferase reporter assay method. The 5′-flanking region of *P2rx2* (a 2524-bp fragment upstream of the putative transcription start site) was inserted into the multicloning site of the pGL3-basic firefly luciferase assay vector (termed pP2X2luc) (Fig. 4A), which was transiently transfected into PC-12 cells. The cloned sequence increased basal luciferase activity by 25-fold. This confirmed that the sequence can promote downstream transcription. When stimulated with 1 μM 9-*cis*-RA, pP2X2luc exhibited higher luciferase activity (from 25.7 ± 2.1 to 42 ± 2.0, 65% increase; $n = 8$; ***, $p < 0.001$) (Fig. 4B). A similar increase in the luciferase activity was also observed with atRA (from 25.7 ± 2.1 to 34.8 ± 2.9., 35% increase; $n = 8$; ***, $p < 0.001$). These results indicate that 9-*cis*-RA and atRA increase the promoter activity of the cloned 5′-flanking region of *P2rx2*. Furthermore, the increases in luciferase activity by 9-*cis*-RA and atRA were lost in cells transfected with a vector lacking the fragment from −2524 to −1924 (Del-pP2X2luc) where three putative RAREs are located (Fig. 4A). In addition, the pGL3-basic vector without the 5′-flanking region of *P2rx2* showed no transcriptional activity, the RAR agonists caused no change, and basal activity of Del-

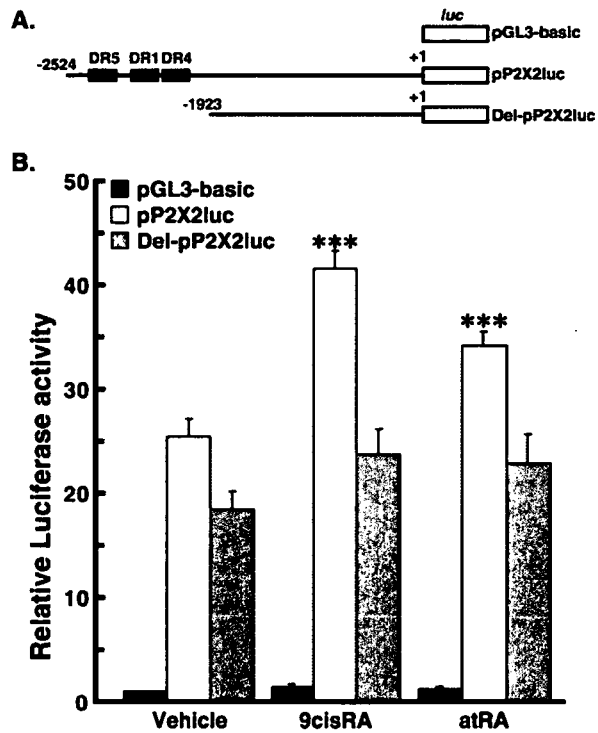

Fig. 4. Transcriptional activity of the 5′-flanking region of *P2rx2* by retinoic acids. The two constructed vectors (pP2X2luc and Del-pP2X2luc) and the empty vector (pGL3-basic) used in the experiment, as described under *Materials and Methods*, are schematically illustrated. Each construct was transfected into PC-12 cells, and the firefly luciferase activity, normalized to the *R. reniformis* luciferase activity driven by the cotransfected phRL-TK, was determined 24 h after the transfection in the presence or absence of 1 μM 9-*cis*-RA or 1 μM atRA (pGL3-basic, open columns; pP2X2luc, closed columns; and Del-pP2X2luc, gray columns). Each value represents the mean ± S.E.M. of the relative light activities to the control treated pGL3-basic vector activity ($n = 8$; ***, $p < 0.001$ by Student-Newman-Keuls method after two-way ANOVA, compared with the value of control group).

pP2X2luc was decreased to 19-fold greater than pGL3, compared with 25-fold grater than pGL3 for pP2X2luc. These results indicate that the RAREs mediate the transcriptional activity of the 5'-flanking region of the *P2rx2* by retinoids.

The Protein Level of $P2X_2$ in PC-12 Cells Is Increased by 9-*cis*-RA Treatment. To investigate whether 9-*cis*-RA increases the level of $P2X_2$ protein as a consequence of an increase in the mRNA level, we performed Western blot analyses to detect $P2X_2$ protein by using a specific antibody for the $P2X_2$ receptor. The specificity of antibody was confirmed by comparing protein blots of 1321N1 cells transfected or untransfected with rP2X2-GFP. In cells transfected with rP2X2-GFP, a single band is detected at approximately 90 kDa, consistent with the molecular mass sum of $P2X_2$ and GFP, whereas no band was detected in untransfected cells. In PC-12 cells, the antibody detected an intense band at approximately 70 kDa with a weak smear ranging from 60 to 80 kDa that was postulated to be glycosylated $P2X_2$ protein. In PC-12 cells that had been treated with 9-*cis*-RA (1–1000 nM) for 24 h, the $P2X_2$ protein was significantly increased in a concentration-dependent manner up to approximately 65% (n = 4–14; *, $p < 0.05$, **, $p < 0.01$) (Fig. 5) in comparison with the level expressed in control. The increase in the $P2X_2$ receptor protein by 9-*cis*-RA was consistent with that in $P2X_2$ mRNA.

9-*cis*-RA Increased the Amplitude of ATP-Evoked Whole-Cell Current in PC-12 Cells. $P2X_2$ receptors form nonselective cation channels, and ATP evokes an inward current (North, 2002). Thus, to investigate whether 9-*cis*-RA increases the level of $P2X_2$ receptors in PC-12 cells as functional channels, we performed whole-cell patch-clamp recordings to examine the ATP-activated inward current. Treatment of cells with 100 nM 9-*cis*-RA for 24 h significantly increased the amplitude of the ATP-evoked inward current (**, $p < 0.01$; Fig. 6, A and B). The concentration-response curves for the ATP-activated currents in control and 9-*cis*-RA-treated cells showed that 9-*cis*-RA did not change the Hill coefficient (control cells, 1.9; 9-*cis*-RA-treated cells, 2.1) and EC_{50} value (control cells, 33; 9-*cis*-RA-treated cells, 30) but enhanced the maximal response (Fig. 6B). Furthermore, 20 μM PPADS almost completely blocked ATP-induced current, which means PPADS-insensitive $P2X_4$ expression is too low to evoke the whole cell current, even though mRNA expression is detectable by RT-PCR. The membrane capacitance, reversal potential, inward rectification property (data not shown), and activation kinetics estimated from the current trace were not significantly changed in the 9-*cis*-RA-treated cells, compared with untreated controls. These results indicate that the expression of functional $P2X_2$ receptors is increased on the plasma membrane of 9-*cis*-RA-treated PC-12 cells.

9-*cis*-RA Facilitates P2X-Mediated $[Ca^{2+}]_i$ Elevation. $P2X_2$ receptors are reported to be highly permeable to Ca^{2+} (Virginio et al., 1998). We monitored the level of $[Ca^{2+}]_i$ in individual PC-12 cells using the Ca^{2+}-sensitive fluorescent

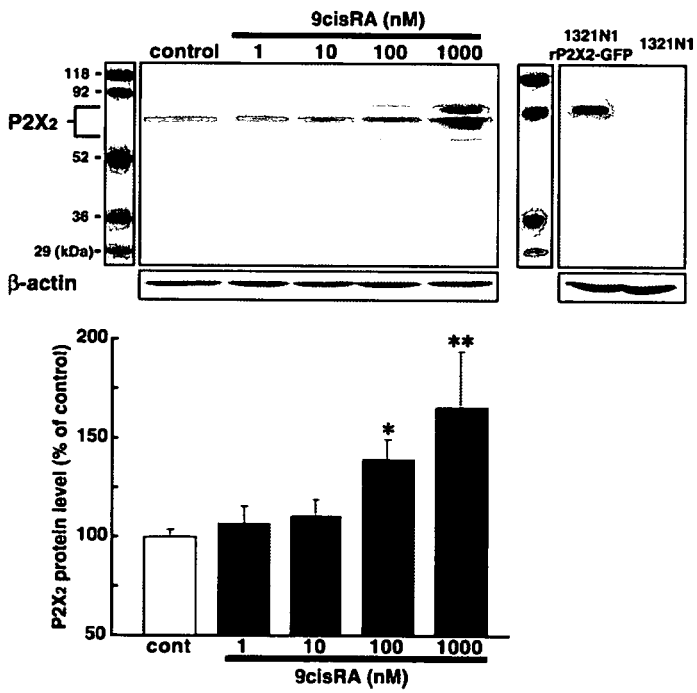

Fig. 5. Increase in $P2X_2$ protein expression by 9-*cis*-RA. Total protein from PC-12 cells treated with or without 9-*cis*-RA (range 1–1000 nM) for 24 h was subjected to Western blot analysis. The proteins of $P2X_2$ receptor and β-actin were detected by their specific antibodies. The intensities of the bands were quantified, and the relative values of $P2X_2$ protein were normalized by the values of the β-actin protein levels for the loading control. The anti-$P2X_2$ antibody was tested on the lysate of 1321N1 cells with or without transfection of P2X2-GFP expression vector. Each set of data represents the mean ± S.E.M. of the percentage over the control (n = 4–14; *, $p < 0.05$; **, $p < 0.01$ by multiple comparisons versus control group using Bonferroni t test after one-way ANOVA).

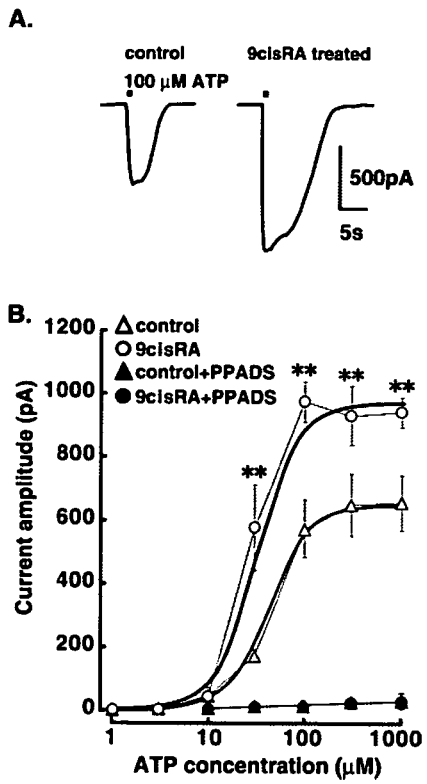

Fig. 6. Effect of 9-*cis*-RA on ATP-induced whole cell current in PC-12 cells. A, representatives traces were the currents evoked by 100 μM ATP in PC-12 cells with or without 100 nM 9-*cis*-RA for 24 h. Cells were voltage-clamped at −60 mV. B, concentration-dependent curves were made by measuring currents elicited by a series of ATP concentrations with or without 20 μM PPADS. Each point represents the mean values ± S.E.M. of the maximum amplitude of the ATP-evoked currents (n = 10–13; **, $p < 0.01$ by t test, compared with the value of the corresponding control group) and was fitted to a sigmoidal curve to calculate Hill coefficient and the EC_{50} values.

dye fura-2 and examined the effects of 9-*cis*-RA on the ATP-evoked $[Ca^{2+}]_i$ elevation. Applying 100 μM ATP produced an increase in the 340/360 emission ratio for fura-2 (n = 21 cells), indicating that ATP caused an increase in $[Ca^{2+}]_i$ in the PC-12 cells (Fig. 7A), as shown previously (Fasolato et al., 1990). Treatment of the cells with 100 nM 9-*cis*-RA for 24 h significantly enhanced the ATP-evoked increase in $[Ca^{2+}]_i$ by approximately 30% (**, $p < 0.01$) (Fig. 7, A and B). PC-12 cells express not only $P2X_2$ but also P2Y (presumably $P2Y_2$) receptors (Raha et al., 1993), both of which increase $[Ca^{2+}]_i$ after their activation. It has been shown that the P2X and P2Y receptor-mediated $[Ca^{2+}]_i$ elevations can be distinguished by using an extracellular recording solution (BSS) without Ca^{2+} to remove P2X component and by treating cells with the phospholipase Cβ inhibitor U-73122 to remove the P2Y component. When Ca^{2+} was not added to the extracellular solution, the increase in $[Ca^{2+}]_i$ evoked by ATP was markedly reduced by ~55% (n = 24 cells) (Fig. 7B). On the other hand, U-73122 (5 μM) reduced the ATP-evoked increase in $[Ca^{2+}]_i$ by approximately 40%. PC-12 cells that had been treated with 9-*cis*-RA did not show any enhancement of the ATP-evoked $[Ca^{2+}]_i$ elevation in the extracellular recording solution without Ca^{2+} but did after treatment with U-73122 (Fig. 7B). Furthermore, inhibition of $P2X_2$ but not $P2X_4$ by 20 μM PPADS reduced ATP-evoked $[Ca^{2+}]_i$ elevation to the level in Ca^{2+}-free BSS both in 9-*cis*-RA-treated or untreated PC-12 cells (Fig. 7B). This result suggests ATP-evoked Ca^{2+} influx through P2X receptors does not include a $P2X_4$ response. Application of 80 mM K^+ evoked the release of DA presumably via activating voltage-dependent Ca^{2+} channels (VDCCs) (Waterman, 2000), but the $[Ca^{2+}]_i$ elevation evoked by 80 mM K^+ was not altered by the treatment with 9-*cis*-RA (Fig. 7B). Together, these results indicate that 9-*cis*-RA up-regulates the expression of $P2X_2$ receptors in PC-12 cells, and activating them by ATP increases Ca^{2+} influx, which contributes to enhancing the neurotransmitter release.

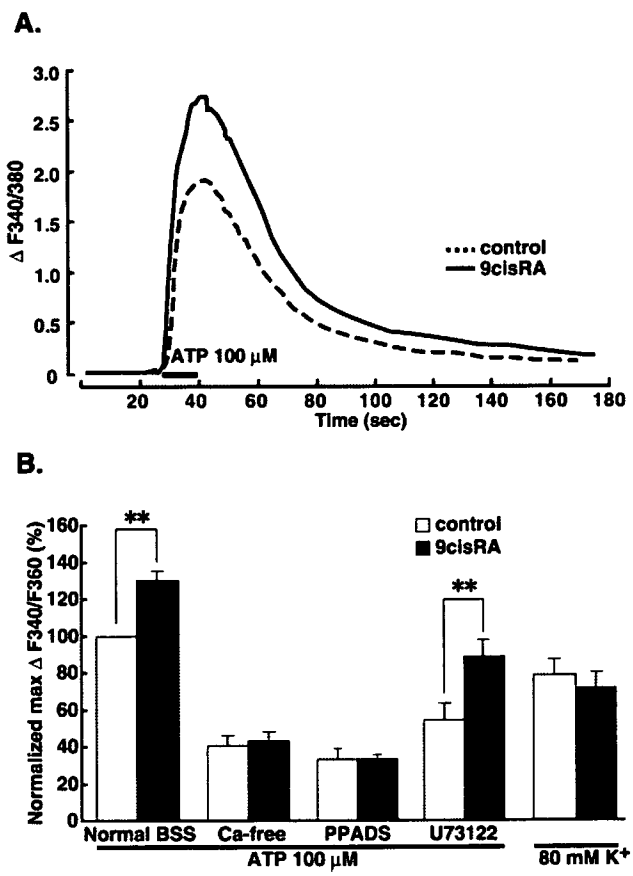

Fig. 7. Effect of 9-*cis*-RA on ATP-induced $[Ca^{2+}]_i$ elevation in PC-12 cells. A, traces showing the records of the fura-2 emission ratios from PC-12 cells onto which 100 μM ATP was applied with or without 100 nM 9-*cis*-RA for 24 h. B, ATP-induced $[Ca^{2+}]_i$ elevations were measured in several different conditions (from left: normal BSS, n = 9; Ca^{2+}-free BSS, n = 5; 20 μM PPADS, n = 3; and 5 μM U-73122, n = 6). To measure the $[Ca^{2+}]_i$ elevation by the depolarizing stimulation, BSS containing a high concentration of potassium (80 mM; n = 5) was applied. Each set of data represents the mean ± S.E.M. of the maximum responses of the ratiometric fura-2 fluorescence ($\Delta F_{340}/\Delta F_{360}$), which were normalized by the value obtained from control PC-12 cells (**, $p < 0.01$ by Student-Newman-Keuls method after two-way ANOVA, compared with the value of control group).

ATP-Induced DA Release from PC-12 Cells Is Enhanced by 9-*cis*-RA Treatment. PC-12 cells are known as a model of neuronal cells (Shafer and Atchison, 1991) and are able to release neurotransmitters such as catecholamines by various extracellular stimuli, including ATP (Nakazawa and Inoue, 1992). The ATP-evoked DA release requires Ca^{2+} influx into cells mediated through opening $P2X_2$ receptor channels but not VDCCs (Inoue et al., 1989). Thus, we investigated whether the ATP-evoked release of DA from PC-12 cells is modulated by 9-*cis*-RA. Stimulation of PC-12 cells with 30 μM ATP for 1 min caused the release of DA as shown previously (Nakazawa and Inoue, 1992). By contrast, in PC-12 cells treated with 100 nM 9-*cis*-RA for 24 h, the ATP-evoked DA release was significantly enhanced by 35.7 ± 7.3% (n = 9; ***, $p < 0.001$; Fig. 8A) without significant change in the total DA content in the cells (94.4 ± 2.4%; p = 0.07; Fig. 8B). 9-*cis*-RA did not affect the spontaneous release of DA from PC-12 cells (control cells, 7.7 ± 2.5%; 9-*cis*-RA-treated cells, 12.8 ± 3.1%; p = 0.23; Fig. 8A).

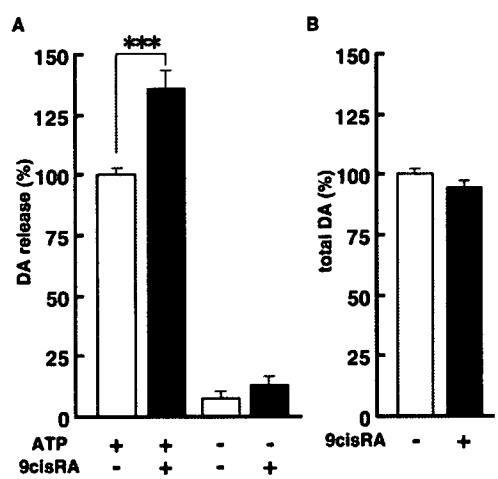

Fig. 8. Enhancement of ATP-evoked dopamine release from PC-12 cells by 9-*cis*-RA. PC-12 cells were incubated with or without 9-*cis*-RA for 24 h. A, the extracellular contents of DA after the application of 30 μM ATP for 1 min were measured with the high-performance liquid chromatography combined with electrochemical detection system. B, measured amount of extracellular and intracellular DA was compared as percentage of 9-*cis*-RA untreated cells. Amount of DA released by ATP was calculated by dividing supernatant values by the sum of supernatant and pellet values and shown as the mean ± S.E.M. of the percentage of the ATP-evoked DA release in 9-*cis*-RA-untreated control cells (n = 9; ***, $p <$ 0.001 by t test).